



On the performance of the snow model Crocus driven by in situ and reanalysis data at Villum Research Station in northeast Greenland

Daniela Krampe¹, Frank Kauker^{1,2}, Marie Dumont³, Andreas Herber¹

5 ¹ Alfred-Wegener-Institut Helmholtz-Zentrum für Polar- und Meeresforschung, Bremerhaven, Germany

² Ocean Atmosphere Systems GmbH, Hamburg, Germany

³ Univ. Grenoble Alpes, Université de Toulouse, Météo-France, CNRS, CNRM, Centre d'Études de la Neige, 38000 Grenoble, France

10 *Correspondence to:* Daniela Krampe (Daniela.Krampe@awi.de)

Abstract. Reliable and detailed snow data are limited in the Arctic. We aim at overcoming this issue by addressing two questions: (1) Can the reanalysis ERA5 replace limited in situ measurements in high latitudes to drive snow models? (2) Can the Alpine model Crocus simulate reliably Arctic snow depth and stratigraphy? We compare atmospheric in situ measurements and ERA5 reanalysis and evaluate simulated and measured snow depth, density and specific surface area (SSA) in northeast Greenland (October 2014–October 2018). To account for differences between Alpine and Arctic region, we introduce a new parametrisation for the density of new snow.

Our results show a good agreement between in situ and ERA5 atmospheric variables except for precipitation, wind speed and direction. ERA5's resolution is too coarse to resolve the topography in the study area adequately, leading presumably to the detected biases. Nevertheless, measured snow depth agrees better with ERA5 forced simulations than forced with in situ measurements.

Crocus can simulate satisfactory the evolution of snow depth, but simulations of SSA and density profiles for both forcings are biased compared to field measurements. Adjusting the new snow density parametrisation leads to improvements in the simulated snow stratigraphy. In conclusion, ERA5 can be used instead of in situ measurements to force snow models but the use of Crocus in the Arctic is affected by limitations likely due to the missing vertical water vapour transport and snow redistribution during strong winds. These limitations strongly affect the accuracy of the vertical profiles of physical snow properties.

1 Introduction

The availability of snow data, especially snow depth and physical snow properties in the Arctic, is temporally and spatially limited. However, snow plays a crucial role in the Arctic, as it covers the ground most of the year as well as the sea-ice during the cold season. Snow depth, snow cover duration as well as snow properties such as density, specific surface area (SSA: Ice-air interface surface area divided by snow mass used instead of grain size, (Calonne et al., 2020)), thermal conductivity and albedo have climatic, ecology and socioeconomic impacts (Callaghan et al., 2011; Sturm et al., 1997; Box et al., 2012; Hall,



2004). Changes in snow cover alter the exchange of energy and mass e.g. by modifying the albedo of the surface as well as the sensible, latent and ground heat fluxes and thus also the length of the growing season (Stiegler et al., 2016). Snow affects the flora and fauna. It is an important habitat for Arctic animals from the smallest like lemmings to the biggest animals the polar bears (Boelman et al., 2019; Liston et al., 2016; Schmidt et al., 2012; Domine et al., 2018).

Despite its importance, the description of snow in current models, e.g. sea ice-ocean models, is very simple as in most cases a fixed density for all layers is assumed (e.g. Uotila et al. (2019)). These simplifications strongly limit the value of the output of these systems. In addition, for numerical weather predictions more accurate snow models allowing for snow metamorphism that work not only in the mid latitudes but also in the Arctic are strongly needed to represent high-latitude – mid latitude linkages that affect the weather over e.g. Europe. Coupling of already existing snow models could help to overcome these issues.

Snow models like Crocus, Snowpack and SnowModel are important tools to gain information about the snowpack evolution where snow measurements are seldom (Bartelt and Lehning, 2002; Liston and Elder, 2006; Vionnet et al., 2012). One snow model used in the Arctic is Crocus, which was originally developed for applications in the European Alps (Vionnet et al., 2012). For this study, we use the snow model Crocus due to the implementation of light absorbing impurities and related processes in snow in the model (Tuzet et al., 2017), which we aim to use for future studies.

The assessment of the performance of Crocus in the Arctic in former studies is contradictory; some studies obtained promising results for Arctic snow properties (Essery et al., 2016; Gouttevin et al., 2018; Sauter and Oblaitner, 2015) while other studies found deficiencies in simulated properties especially for snow density and snow conductivity (Barrere et al., 2017; Domine et al., 2019; Domine et al., 2016b). Challenges arrive due to the different atmospheric conditions causing considerably different snow characteristics for the Arctic and the European Alps. Snowpacks in the European Alps are warmer and deeper than in the Arctic. In addition, Alpine snow is close to its melting point and melting occurs frequently (Jacobi et al., 2010; Essery et al., 2016). Furthermore, colder air temperatures and the absence of direct radiation in winter lead to huge temperature gradients that determine the stratigraphy of Arctic snowpacks. Adjustments of the original model can help to overcome these differences (Jacobi et al., 2010; Sauter and Oblaitner, 2015; Barrere et al., 2017).

However, complete and sufficiently long time series of meteorological measurements, especially reliable precipitation data, to force these models are limited in the Arctic (Boelman et al., 2019). Therefore, snow models are often driven by atmospheric reanalysis delivering complete time series of meteorological data for given locations or areas (Barrere et al., 2017; Domine et al., 2019; Gouttevin et al., 2018). Such reanalysis data are physically consistent, which cannot be guaranteed for in situ observations (Hersbach et al., 2020). Starting in 2016, data from the next generation global atmospheric reanalysis ERA5 (European Centre for Medium-Range Weather Forecasts (ECMWF) ReAnalysis-5th Generation (ERA5) atmospheric reanalyses data set) are available (Hersbach et al., 2020). Some studies already evaluated the performance of ERA5 in the Arctic (Delhasse et al., 2020a; Wang, 2019). However, more studies are needed to investigate strengths and weaknesses of the reanalysis accurately. So far, nobody used ERA5 to force the snow model Crocus in the Arctic and investigated their performance for the coastal region in northeast Greenland.



The overall objective of this paper is to evaluate the performance of the snow model Crocus driven by in situ and reanalysis data for Greenland. In particular, we aim to answer two main questions: (1) Can the reanalysis ERA5 replace in situ measurements where in situ data is limited? (2) Can we apply the Alpine snow model Crocus in the Arctic to obtain reliable snow depth evolution and other physical snow properties as, e.g. the vertical profiles of snow density and SSA.

For this study we use in situ observations from Greenland at Villum Research Station, where both meteorological data and snow depth were measured. In addition, during a campaign in spring 2018 numerous snow parameters, as snow depth, snow density and SSA were measured.

2 Methods

We investigated the potential of using the atmospheric reanalysis ERA5 to force the snow model Crocus by comparing the needed near surface data to meteorological in situ measurements at Villum Research Station. We further evaluated the performance of Crocus to simulate physical snow properties at this high Arctic location.

The study area is located in the surroundings of the atmospheric measurement mast of Villum Research Station (81°34' N, 16°38' W, 37 m above sea level) (hereafter Villum Research Station) in northeast Greenland (Fig. 1). The Wandel Sea in the north, a local ice cap called Flade Isblink in the south and east and fjords in the west surround the low land, which consists of continuous permafrost with an active layer of 20 cm in maximum. The observed annual mean temperature is -21°C and the annual precipitation is 188 mm (Rasch et al., 2016).

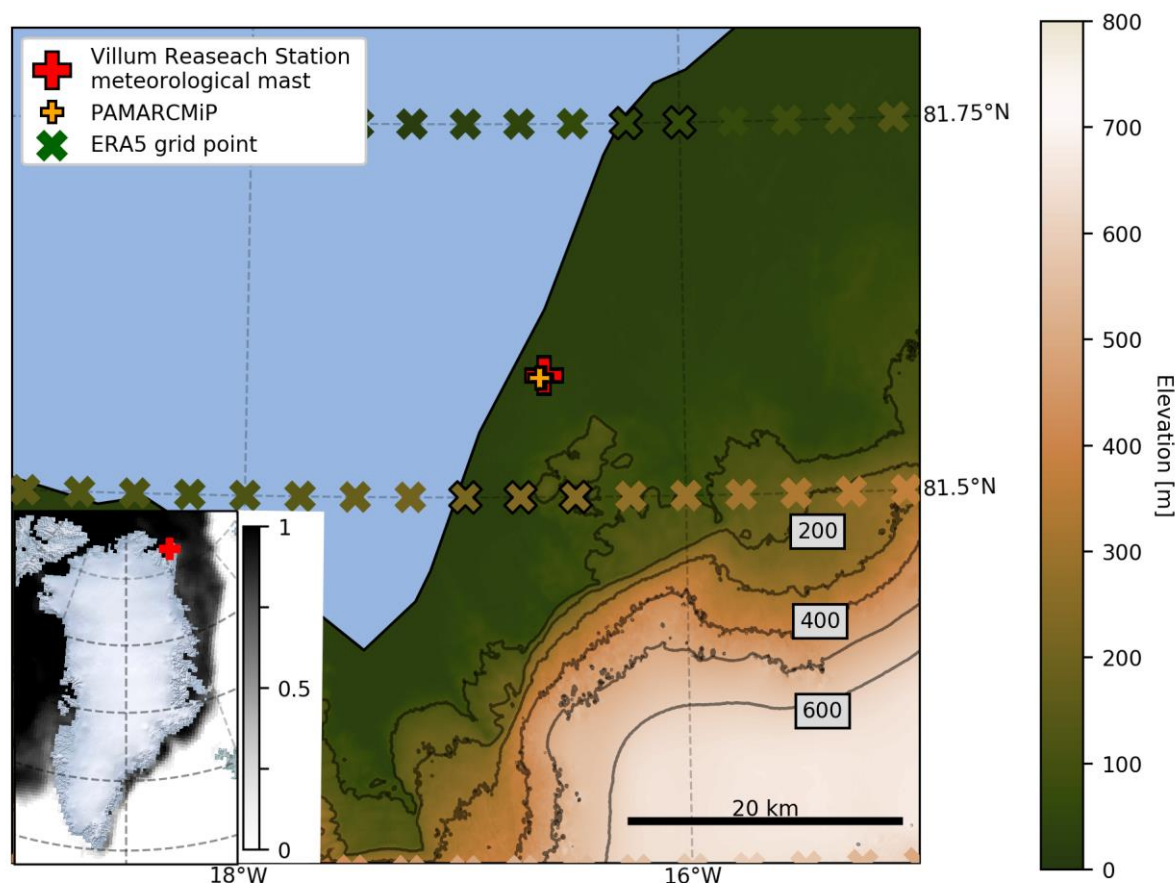


Figure 1: Map showing location of meteorological mast of Villum Research Station (red cross), measurement location during PAMARCMiP (yellow cross), ERA5 grid cells (green crosses) and terrain elevation in northeast Greenland (Digital elevation model: Howat et al., 2015; Howat et al., 2014). Crosses with black frame are the ERA5 grid cells used in the study. Small inserted panel at left bottom: Sea ice concentration from 15 March 2018 (Maslanik and Stroeve, National Snow and Data Center, updated yearly).

2.1 The snow model Crocus

We used the multilayer snow model Crocus (Brun et al., 1992; Vionnet et al., 2012) in single-column mode and evaluated its performance in the Arctic on bare soil. The snow model is embedded in the surface scheme SURFEX and is coupled with the soil model ISBA-DF (Boone et al., 2000). We use SURFEX version 8.1. The model can deal with up to 50 vertical dynamical snow layers. Layer thickness, heat content, density and age characterise each snow layer. The number of the snow layers is dynamical, i.e. layers can run empty (zero thickness).

Crocus describes the evolution of the snowpack by taking the energy- and mass balance of the snowpack into account. Implemented processes are surface melting, internal melting and refreezing, compaction, snow metamorphism, providing a tracer for snow age, near surface densification and enhanced sublimation as well as fragmentation and compaction due to snowdrift and solar absorption in the snowpack. Snow compaction and microstructural changes due to wind drift in Crocus



occur when wind speed exceeds a transport threshold depending on snow properties. Commonly, this threshold is at 6 m s^{-1} (Vionnet et al., 2013). These wind drift effects are passed on to the underlying layers with an exponential decay until a layer's transport threshold is lower than the wind speed. Snow redistribution is not taken into account (Vionnet et al., 2013). Crocus is driven by surface fluxes calculated from the atmospheric forcing variables air temperature, specific humidity, wind speed, incoming direct and diffuse shortwave and longwave radiation, rain- and snowfall rate and surface air pressure. In addition to the atmospheric forcing, the model uses the terrain information aspect, slope and altitude as well as optionally wet and dry deposition coefficients of black carbon or other light absorbing impurities (Tuzet et al., 2017). A detailed description of the model can be found in Vionnet et al. (2012).

2.2 Data

2.2.1 ERA5 reanalysis data

The global atmospheric reanalysis ERA5 is available in the Climate Data Store of Copernicus on a regular latitude-longitude grid at $0.25^\circ \times 0.25^\circ$ resolution, with atmospheric parameters on 37 pressure levels and has a temporal resolution of one hour (Hersbach et al., 2020). For Villum Research Station the grid cell size is 5 km along the longitude and 31 km along the latitude. The output of the simulations driven by ERA5 are representable on spatial scales of at least one grid cell size, i.e. on 5 km x 31 km. Delhasse et al. (2020a) found a good performance for near-surface variables over the Greenland Ice Sheet as well as other studies in snow-covered locations worldwide (Albergel et al., 2018; Wang et al., 2019; Urraca et al., 2018).

Instead of interpolating spatially to the location of Villum Research Station, we took the nearest available grid cell (mid-point at $81.5^\circ \text{ N } 16.75^\circ \text{ W}$, 185 m above sea level), which is about 10 km south from Villum Research Station. This is done to avoid spatial interpolation of the needed atmospheric variables, which might lead to destruct their physical consistency due to non-linearities in the underlying atmospheric process formulation in the model. We ran the model with atmospheric input from four additional nearest grid cells to Villum Research Station located on land (Fig. 1) to account for biases resulting from taking the nearest neighbour. The results of the additional runs were taken as a metric for the co-location error, i.e. were deemed to give information of the representativeness of the ERA5 data (see Loew et al., 2017 for an introduction of the terminology used).

Several data conversions were needed to drive Crocus: (i) ERA5 provides the variables snowfall and precipitation. However, model tests showed a better agreement between simulated and observed snow depths when splitting ERA5's total precipitation rate into liquid and solid precipitation rates after Jennings et al. (2018). Therefore, precipitation at temperatures of 1°C or warmer is handled as liquid precipitation and the residual as snowfall. (ii) Incident shortwave radiation was split into diffuse and direct shortwave radiation using the zenith angle depending on the solar declination, the local time and latitude. (iii) Wind speed and wind direction were calculated from the wind vector and (iv) specific humidity from surface air pressure, temperature and dew point temperature according to Willett et al. (2008).



2.2.2 Meteorological observations

130 Villum Research Station provided meteorological data obtained by an automatic weather station installed in 2014 (Villum Research Station, 2021). Table 1 gives an overview about the installed meteorological sensors and their accuracy. To force Crocus, we resampled the data to obtain hourly mean and accumulated data, respectively, for our study period from 27 November 2015 to 08 August 2018.

135 **Table 1: Meteorological sensors installed at Villum Research Station (ASIAQ, 2014; Yankee Environmental Systems, 2012).**

Variable	Device	Accuracy	Sensor height [m]	Missing measurements
Air temperature	ROTRONIC - HC2-S3C03-PT15	$\pm 0.1^{\circ}\text{C}$	3	1.9 % (450 h)
Relative humidity	ROTRONIC - HC2-S3C03-PT15	$\pm 1 \%$	3	2.9 % (697 h)
Wind speed	Vector Instrument - A100R	$\pm 0.1 \text{ m s}^{-1}$	9	5.9 % (1395 h)
Wind direction	Vector Instrument - W200P	$\pm 2^{\circ}$	9	5.1 % (1229 h)
Surface air pressure	Vaisala - PTB110	$\pm 1.0 \text{ hPa}$	2	1.4 % (330 h)
Incoming shortwave radiation	Kipp&Zonen - CNR4	$< 5 \%$	3	19.0 % (4499 h)
Incoming longwave radiation	Kipp&Zonen - CNR4	$< 10 \%$	3	5.6 % (1324 h)
Precipitation	Yankee Environmental Systems - TPS-3100	$\pm 0.5 \text{ mm h}^{-1}$	3	35.2 % (8326 h)

We used ERA5 data to fill in missing data for all variables, except for precipitation, as especially the amount and timing of strong precipitation events were too diverse between ERA5 and in situ measurements. In addition, an overestimation of precipitation was introduced when filling missing precipitation data with ERA5 precipitation, most likely because of the different spatial scales of precipitation in ERA5 and the in situ data (the latter containing much smaller scales). Therefore, we set missing precipitation data to zero deliberately introducing a potential underestimation of the accumulated precipitation. Most of the surface input variables required by Crocus were measured directly. However, some conversions had to be carried out to get all required forcing variables in the appropriate form: (i) Precipitation was split in liquid and solid phase after Jennings et al. (2018), as it was done for the ERA5 precipitation (Sect. 2.3.1). (ii) The zenith angle depending on the solar declination, the local time and latitude is used to separate incident shortwave radiation into diffuse and direct shortwave radiation. (iii) The Magnus-equation (Magnus, 1844) is applied to calculate specific humidity from the measured surface air pressure, air temperature, and relative humidity.

2.2.3 Validation data

We evaluated the model performance by comparing simulated and measured snow depth, snow density and SSA (Table 2). In situ snow depth was measured at Villum Research Station from 26 August 2014–30 September 2018 (ASIAQ, 2014). As second validation dataset we used in situ data obtained during the Polar Airborne Measurements and Arctic Regional Climate Model Simulation Project (PAMARCMiP) campaign, in a distance less than 500 m away from Villum Research Station, between 10 March and 08 April 2018. Measurements included, snow density, SSA and snow depth.



155 Vertical profiles of snow density and SSA were retrieved from a SnowMicroPen (SMP), a snow penetrometer measuring the
 bonding force between snow grains with a vertical resolution of 1.25 mm (Schneebeli et al., 1999). While the density retrieved
 from SMP measurements was calculated following Calonne et al. (2020), Proksch et al. (2015) and King et al. (2020), SSA
 was obtained based on Calonne et al. (2020) and Proksch et al. (2015), as King et al. (2020) did not provide any SSA
 160 parametrised. After comparing the results for all parametrisations, we used results after Calonne et al. (2020) (see Sect. 4.2.2
 for discussion). Due to thick ice layers within the snowpack, the SMP could not penetrate the full vertical profile and snow
 depth measurements were not possible. To keep, a comparable snow depth between SMP measurements and simulation results,
 we used the latter as reference height (maximum 2.4 m during PAMARCMiP campaign) also for the SMP measurements.
 In addition, on 03 April 2018, snow depth was measured with a ruler, and every 10 cm of the profile, snow density with a
 density cutter (60x30x56 mm) and SSA with an IceCube3. The optical system IceCube measures the hemispherical infrared
 165 reflectance of snow and converts the reflectance in SSA (Zuñon, 2013).

Table 2: Instruments used to measure snow physics at Villum Research Station and during PAMARCMiP campaign to validate Crocus.

Variable	Device	Accuracy	Measurement date
Snow depth	Campbell - SR50A	±1 cm (ASIAQ, 2014)	26 Aug 2014–30 Sep 2018
Snow density and specific surface area	SnowMicroPen	Arctic mean relative error ~15 % (from Proksch et al. (2015), note that here we use Calonne et al. (2020), but no accuracy is delivered by Calonne et al.	23 March 2018
Snow density	Density Cutter	±10 % (Domine et al., 2016a)	03 April 2018
Specific surface area	IceCube3	±10 % (A2 Photonic Sensors, 2016)	03 April 2018

2.3 Adaptation of Crocus: New snow density parametrisation

170 The original parametrisation of the density of new (freshly fallen) snow, ρ_{new} within Crocus (hereafter V12) formulated for
 the European Alps is:

$$\rho_{\text{new}} = a_p + b_p (T_a - T_{\text{fus}}) + c_p U^{1/2}, \quad (1)$$

175 where T_a is the air temperature, T_{fus} is the melting point temperature for water, U is the wind speed and a_p is 109 kg m^{-3} , b_p is
 $6 \text{ kg m}^{-3} \text{ K}^{-1}$, and c_p is $26 \text{ m}^{-7/2} \text{ s}^{-1/2}$ (Vionnet et al., 2012). Figure 2a shows the dependency of the new snow density using V12
 on wind speed and air temperature. With this linear dependence on temperature the new snow density becomes negative for
 temperatures below -30°C . To avoid negative and unrealistic small new snow densities, the minimum new snow density is
 originally set to 50 kg m^{-3} . However, this parametrisation was deduced from measurements at Col de Port, French Alps, where



temperatures below -20°C occur seldom (Vionnet et al., 2012). For the Arctic, where temperatures below -20°C are frequent, this parametrisation leads to numerous new snow densities of the minimum density (50 kg m^{-3}) deemed unrealistic for high Arctic conditions. The lowest measured snow density during PAMARCMiP, for instance, was 117 kg m^{-3} . Also other studies found too low new snow densities for the Arctic simulated with Crocus (Essery et al., 2016; Sauter and Oblitner, 2015).

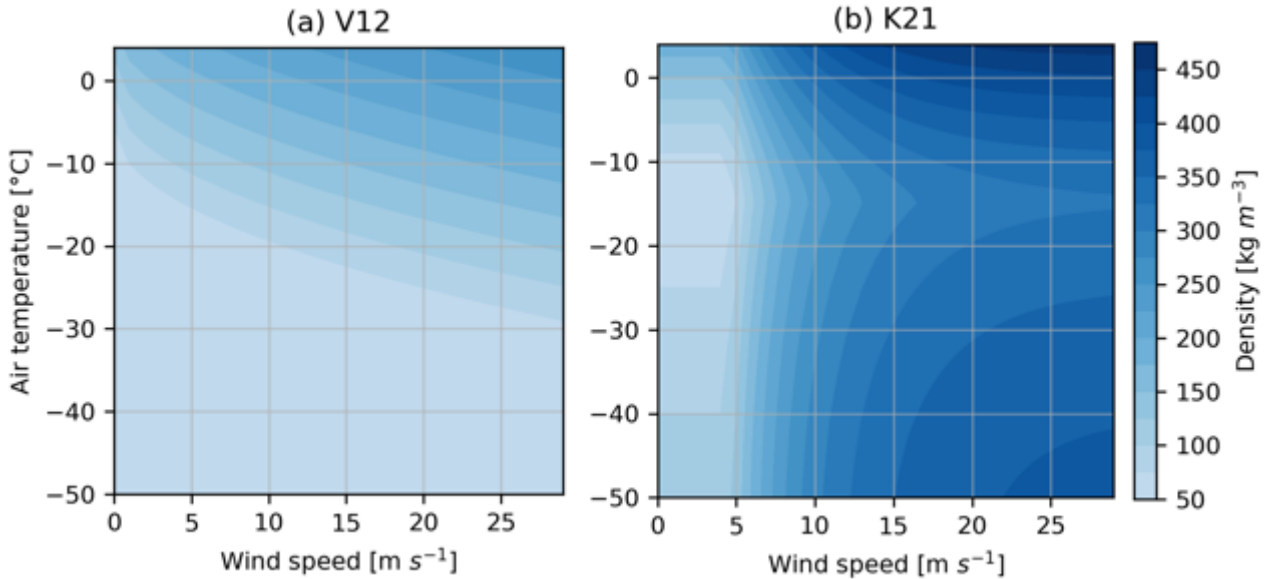


Figure 2: New snow density dependence on wind speed and air temperature for the parametrisation of (a) V12 (original) and (b) K21 (this paper).

Therefore, we aimed to find a new snow density parametrisation suitable for the cold temperatures in the Arctic preferable without an “unphysical” ad hoc cut-off density at low temperatures. We compared the performance of Crocus for alternative new snow density parametrisations from Anderson (1976), Liston et al. (2007), Sauter and Oblitner (2015) and Van Kampenhout et al. (2017) and various adaptations of these parametrisations. The parametrisation of Anderson (1976) does not account for wind influence on new snow density, Liston et al. (2007) is only defined for temperatures above -16°C , while Sauter and Oblitner (2015) used different constants for a_p , b_p and c_p valid for Svalbard. Van Kampenhout et al. (2017) used the same equation to obtain temperature related new snow density for temperatures from -15°C to 2°C as Liston et al. (2007). Based on that, we use for this study a combination of Liston et al. (2007) and Van Kampenhout et al. (2017) as it represents best our observations and needs.

The new snow density parameterisation by Liston et al. (2007) is defined for $T_{wb} \geq 258.16 \text{ K}$ and is given as:

$$\rho_{new_{T \geq -15^{\circ}\text{C}}} = 50 + 1.7(T_{wb} - 258.16)^{1.5}, \quad (2)$$

for wind speed below 5 m s^{-1} , where T_{wb} is the wet-bulb air temperature in Kelvin.



For wind speed $\geq 5 \text{ m s}^{-1}$ the new snow density is defined as:

$$\rho_s = \rho_{newT \geq -15^\circ\text{C}} + \rho_w \quad (3)$$

205 with

$$\rho_w = D_1 + D_2 \{1.0 - \exp[-D_3 (W_t - 5.0)]\}, \quad (4)$$

where D_1 is the density offset of 25.0 kg m^{-3} for a 5.0 m s^{-1} wind, D_2 is the maximum density increase of 250.0 kg m^{-3} caused
 210 by wind and D_3 sets the progression from low to high wind speed and is 0.2 m s^{-1} . W_t is the terrain-modified wind speed at 2 m
 above the surface in m s^{-1} (Liston et al., 2007).

To simplify Eq. (4) we used directly measured wind speed for in situ and given ERA5 wind speed without any terrain
 modifications. Wind speed was measured at 9 m and ERA5 wind speed was calculated for 10 m height. We tested the log law
 and the power law approach to downscale wind speed to 2 m with almost identical results in snow density and snow SSA for
 215 both approaches. Therefore, we present only results for 9 m (in situ) and 10 m (ERA5) wind speeds in this study.

For temperatures below -15°C , we extend the parameterisation by the new snow density parameterisation from Van
 Kampenhout et al. (2017) but keep the wind depended part from Liston et al. (2007):

$$\rho_{sT < -15^\circ\text{C}} = \rho_{newT < -15^\circ\text{C}} + \rho_w, \quad (5)$$

220

with

$$\rho_{newT < -15^\circ\text{C}} = -3.8328 (T - T_{frz}) - 0.0333 (T - T_{frz})^2, \quad (6)$$

where T is the near surface air temperature and T_{frz} is the freezing temperature of water 273.15 K .

225 The parameterisation for temperatures below -15°C from Van Kampenhout et al. (2017) does not consider any dependence on
 humidity. However, the influence of humidity below -15°C should be negligible, as humidity at temperatures below -15°C is
 low. Density inversions at temperatures below -15°C as observed by Van Kampenhout et al. (2017) are taken into account
 with this parameterisation. Figure 2 visualise the different new snow densities obtained with the original parameterisation and
 our adapted parameterisation (hereafter K21).

230 2.4 Model simulations setup

An overview of all model simulations is listed in Table 3. We forced several model simulations with ERA5 data over the
 period from 2010 to August 2020. Due to a constant negative offset throughout the years in the reanalysis surface air pressure,



probably caused by orographic effects (see Sect. 3.1.1), we adjusted ERA5 surface air pressure by adding the mean difference between in situ air pressure and ERA5 air pressure. To reduce spin-up effects, introduced through the initial conditions of the soil, we used the initial conditions on 31 December 2019 after running one ERA5 forced simulation from 2010 to December 2019. This second pass of the forcing period simulation is called ERA5 control run (ERA5-CTRL). ERA5-NSD used the same forcing as ERA5-CTRL but with the introduced new snow density parametrisation K21. Simulations to analyse the impact of simulated snow depth to forcing variables (ERA5-sens) (see Sect. 2.6) used ERA5-CTRL forcing but with a disturbance on each individual forcing variable.

The in situ control simulation (Insitu-CTRL) is forced with the in situ measurements from Villum Research Station from 27 November 2015 to 08 August 2018, except from erroneous measured longwave radiation, which was replaced by the corresponding ERA5 variable for the whole study period. To reduce spin-up effects for the in situ simulation, we used the archived initial conditions from 26 November 2015 of ERA5-CTRL, as initial conditions for the in situ simulation. The in situ simulation using the introduced new snow density parametrisation K21 is called Insitu-NSD.

For all simulations we set the absorption enhancement parameter B_0 to 1.6 in line with other studies (Tuzet et al., 2020; Libois et al., 2013). As we had no measurements for wet and dry black carbon deposition rates, we used results from Tuzet et al. (2020) for the French Alps as indication, but assumed lower rates for northeast Greenland. Therefore, we set wet and dry constant deposition rates to $6.67 \times 10^{-11} \text{ g m}^{-2} \text{ s}^{-1}$ and $3.33 \times 10^{-11} \text{ g m}^{-2} \text{ s}^{-1}$, respectively.

Table 3: Overview of all conducted model simulations (LWdown: Longwave radiation downwards, PSurf: Surface air pressure).

Name of simulation (acronym)	Forcing data	Timeframe	Adaptations
ERA5 control (ERA5-CTRL)	ERA5 data	2010–2020	PSurf offset adapted to in situ data
ERA5 new snow density adapted (ERA5-NSD)	as in ERA5-CTRL	2010–2020	as ERA5-CTRL but new snow density after K21
ERA5 sensitivity (ERA5-sens)	as in ERA5-CTRL	2010–2020	as ERA5-CTRL but one simulation for each forcing variable is disturbed by + one-tens standard deviation
In situ control (Insitu-CTRL)	in situ data, LWdown from ERA5	Nov 2015–Aug 2018	LWdown from ERA5
In situ new snow density adapted (Insitu-NSD)	as Insitu-CTRL	Nov 2015–Aug 2018	as Insitu-CTRL but new snow density after K21

2.5 Sensitivity simulations

To understand the difference between the simulated snow depth obtained from Insitu-CTRL and ERA5-CTRL, respectively, we used a linear approach of partial disturbance. With this approach we were able to figure out the contribution of every forcing variable to the difference in the simulated snow depth.

We used ERA5-CTRL as baseline simulation because of its consistency and completeness of all variables for our sensitivity survey. From the ERA5 data, we calculated the daily standard deviation from 2010 to August 2020 for every forcing variable. We added one-tens of the standard deviation to the individual variable as typical disturbance d_i while all other variables were



unchanged in each simulation of ERA5-sens. Then, we determined the difference between snow depth values retrieved from ERA5-sens and ERA5-CTRL for every simulation with one disturbed forcing variable. The sensitivity $e(x_i)$ for every forcing variable is defined as:

$$e(x_i) = (m(x_i + d_i) - m(x_i)) / d_i, \quad (7)$$

with d_i being one-tens of the standard deviation from the ERA5 i th forcing variable.

We estimated the influence of each forcing variable on the snow depth difference between Insitu-CTRL and ERA5-CTRL as:

$$m(x_i') - m(x_i) = e(x_i)(x_i' - x_i), \quad (8)$$

with $m(x_i') - m(x_i)$ being the mean bias of in situ and ERA5 simulated snow depth and with $x_i' - x_i$ being the mean difference between the i th in situ and the corresponding ERA5 forcing variable. For a perfect linear model, the sum over all forcing variables x_i of $m(x_i') - m(x_i)$ would be equal to the snow depth difference between Insitu-CTRL and ERA5-CTRL. However, because of the non-linear model the sum is an approximation of the “real” difference of both simulations but allows us to identify the main reasons of the difference between Insitu-CTRL and ERA5-CTRL.

3 Results

3.1 Forcing data

3.1.1 Comparison of reanalysis data and in situ measurements from Villum Research Station

Villum Research Station provided meteorological measurements that we compared with ERA5 data to evaluate the performance of the reanalysis for Greenland. We removed the annual cycle from the time series by subtracting the observed monthly mean “climatology” from 27 November 2015 to 08 August 2018 from the observed in situ data and the ERA5 reanalysis, respectively. By analysing these anomalies, we identified the mean biases and correlations between the in situ data and the reanalysis.

Figure 3 shows the comparison of daily anomalies of the atmospheric forcing variables from ERA5 with the in situ data. Observed direct shortwave radiation, diffuse shortwave radiation, specific humidity and air temperature agreed well over the period from 27 November 2015 to 08 August 2018. Mean biases were small and the Pearson correlation coefficients were in the range of 0.84 to 0.91. ERA5 underestimated the air temperature by 1.0°C and the specific humidity by 0.0002 kg kg⁻¹. Longwave radiation showed a poor correlation (r : 0.28) and a high root-mean-square difference (RMSD: 60.5 W m⁻²) explained by a tilt of one of the sensors used to obtain longwave radiation (per. Comm. with Andreas Massling).



Atmospheric surface pressure correlated well with in situ surface pressure ($r: 0.99$) but showed a systematic offset of 19 hPa. We attribute that bias to the altitude difference of the ERA5 nearest grid cell to Villum Research Station of about 150 m due to the relatively coarse resolution of ERA5. ERA5 surface air pressure of the four grid cells closest to Villum Research Station showed a large spread (mean surface air pressure difference -9 hPa, standard deviation: 13 hPa). Grid cells further north had a lower elevation than the grid cells at 81.5°N (Fig. 1).

To account for the offset, we corrected ERA5 surface pressure by the mean difference between in situ and ERA5 over the period. As we used surface pressure to calculate the specific humidity from ERA5's dew point temperature, changes in pressure influenced the specific humidity. However, effects were small.

Rain- and snowfall showed mean biases of 0.1 mm day^{-1} and 0.6 mm day^{-1} w.e. (water equivalent) and poor correlations of 0.15 and 0.13, respectively. Additionally, precipitation measurements were incomplete – for about 35 % of the time no data were available. Observed and ERA5 precipitation differed strongly not only in the amount but also in the timing of extreme events. In situ precipitation was generally higher than ERA5 precipitation. ERA5 rainfall tended to be delayed and weaker than in situ rainfall.



Daily anomalies ERA5 and in situ data

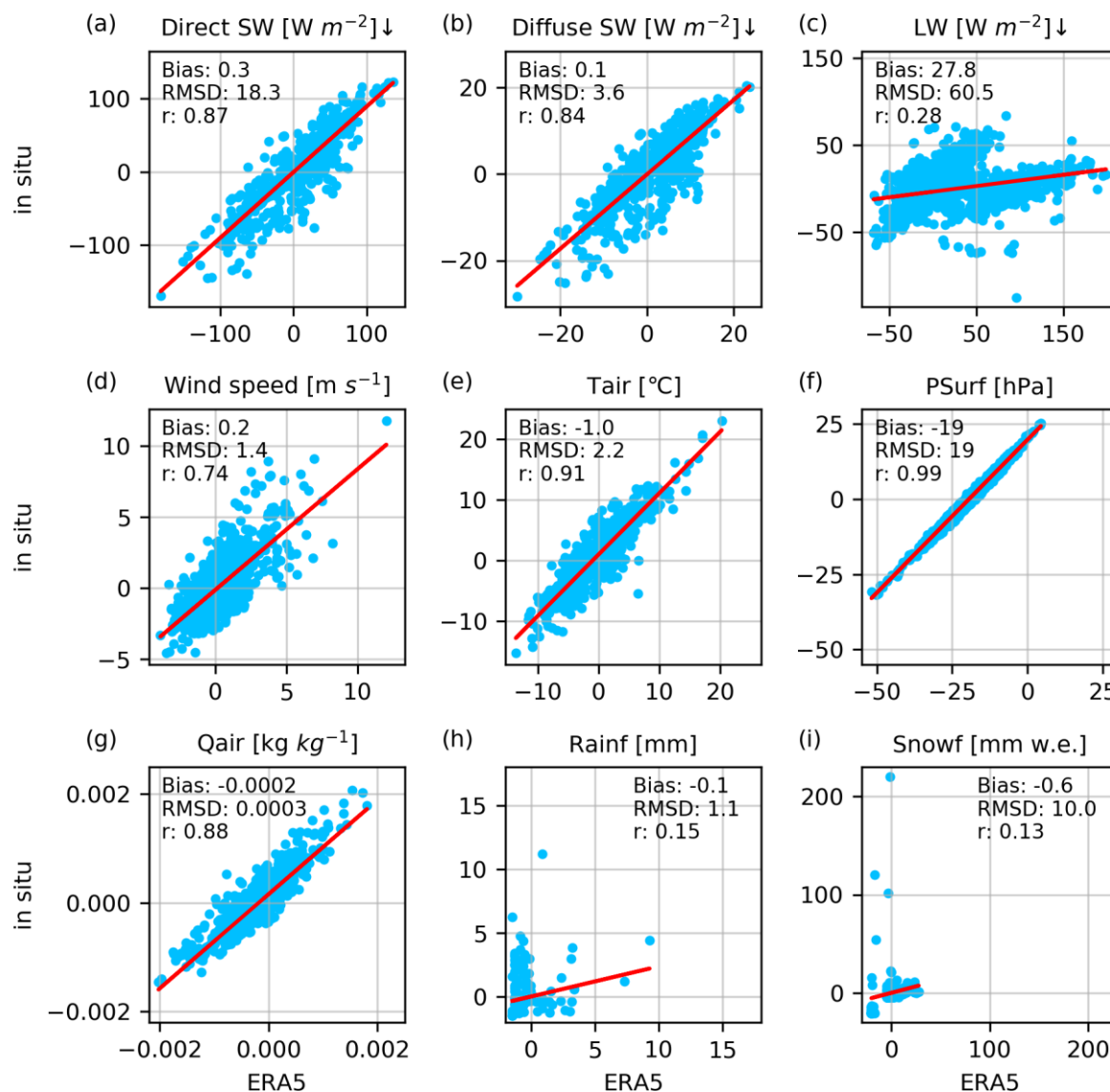
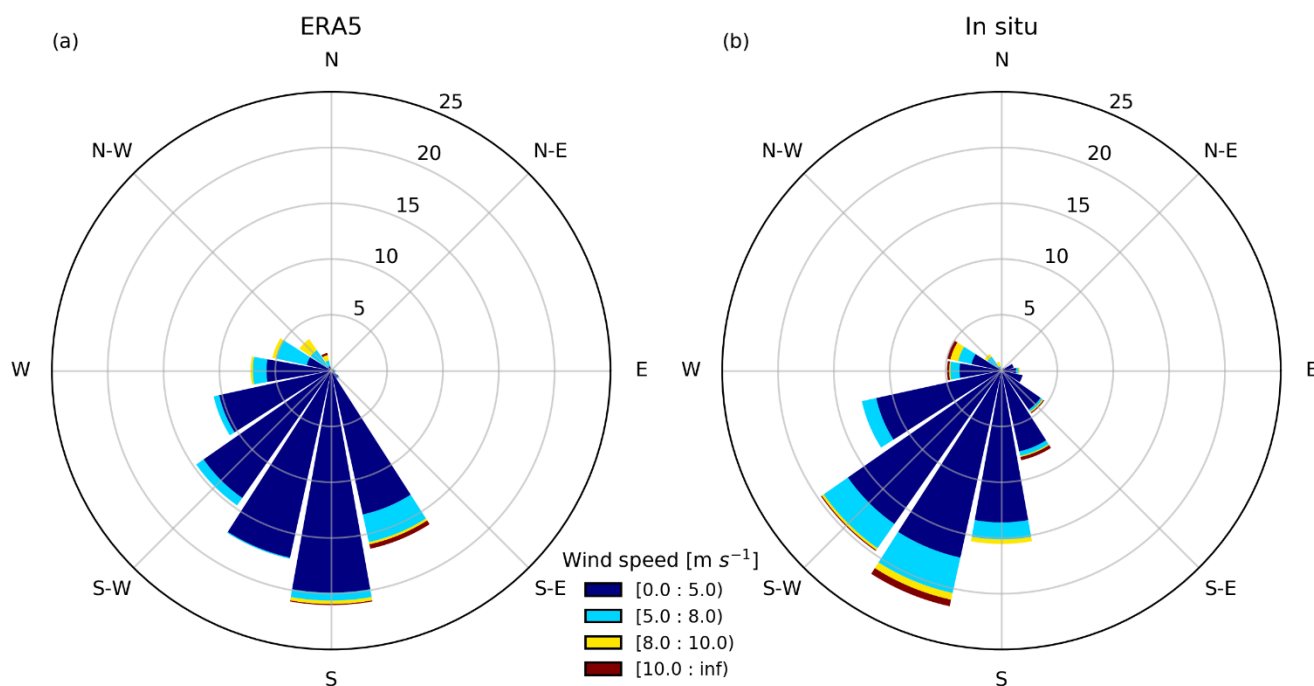


Figure 3: Comparison of ERA5 and in situ daily anomalies. Metric displayed are the mean bias defined as ERA5 – in situ, root mean squared difference (RMSD) and correlation coefficient (r). Blue dots show the values for the variables red lines the regression line. (a) Direct incoming shortwave radiation (SW), (b) diffuse incoming SW, (c) incoming longwave radiation (LW), (e) air temperature (Tair), (f) surface air pressure (PSurf), (g) specific humidity (Qair), (h) rainfall (Rainf) and (i) snowfall (Snowf) in mm w.e. (water equivalent).

ERA5 and measured wind direction show large deviations. Measured preferred wind direction was from the south-west while ERA5's preferred wind direction was from the south (Fig.4). Also, wind direction for wind speeds higher than $5 m s^{-1}$, which



310 potentially lead to snow redistribution due to wind drift, differed considerable. The mean wind speed from ERA5 over the whole study period was slightly higher than measured (0.2 m s^{-1}). However, ERA5 underestimated the occurrence of wind speeds higher than 5 m s^{-1} .



315 **Figure 4: Daily mean wind speed and wind direction for (a) ERA5 data and (b) in situ data. Wind speed is indicated by colour, numbers represent the frequency of wind direction occurrence in percent.**

3.1.2 Atmospheric conditions during and shortly before the PAMARCMiP campaign

In the second half of February 2018 there was a remarkable period of exceptional weather conditions lasting about two weeks (Fig. 5), where even air temperatures above freezing temperature were present in hourly data (Moore et al., 2018; Ludwig et al., 2019). The mean daily air temperatures between 17 Feb 2018 and 27 Feb 2018 were about 20°C warmer than in the weeks before and after. During PAMARCMiP itself, air temperature was about -20°C .

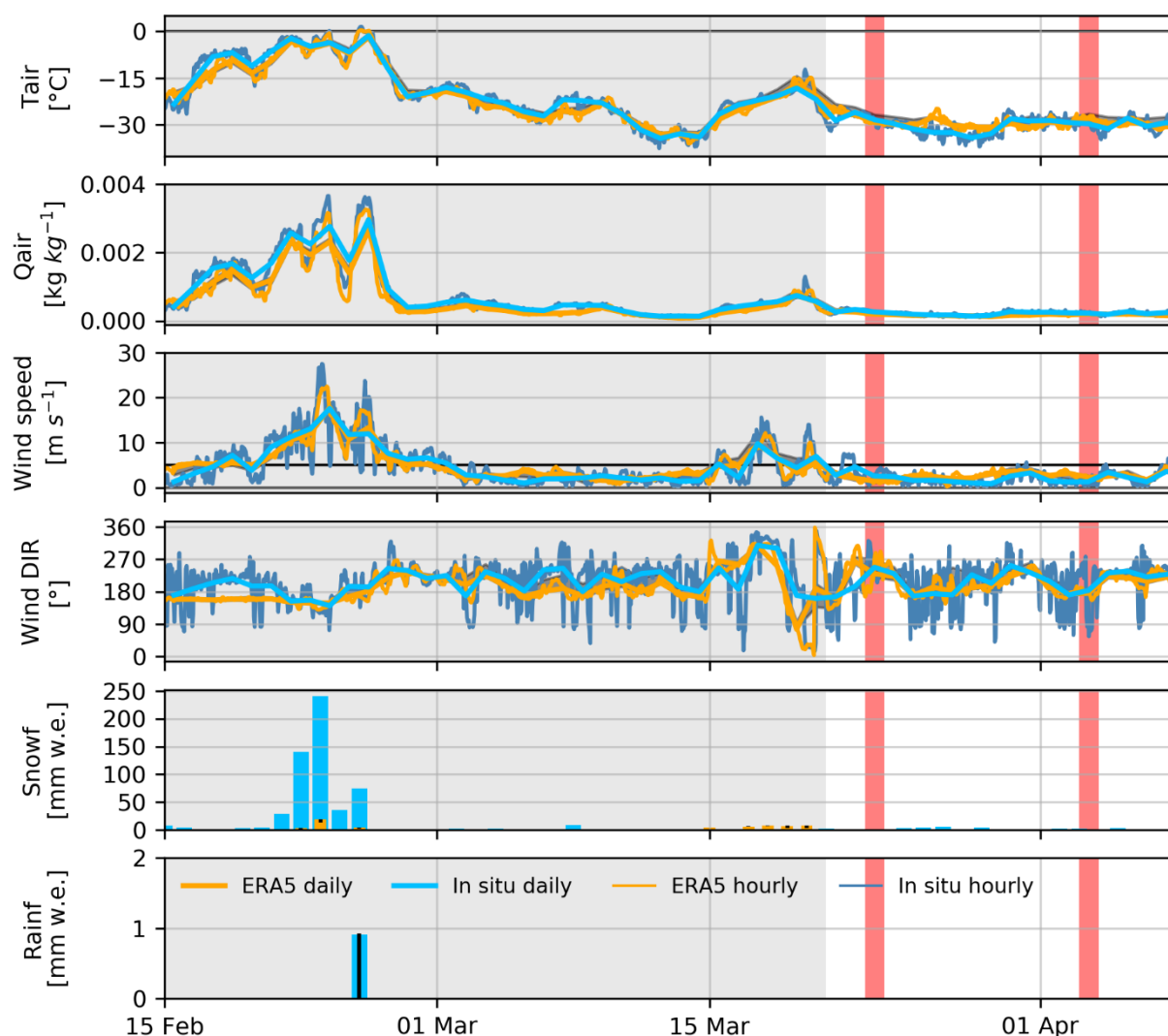
320 The warm event was accompanied by remarkable strong winds, which were above the wind drift mark of 5 m s^{-1} . Hourly in situ wind speeds exceeded 20 m s^{-1} . During the time of the snowpit survey observed wind speeds were slightly below 5 m s^{-1} with some hours above 5 m s^{-1} at the beginning of the campaign. During the warm and strong wind event, wind direction was
 325 mainly south to southeast, shifting towards southwest afterwards.

ERA5 underestimated snowfall during the first warm event by more than five times. Due to the short periods of air temperature above the freezing temperature there was also some rainfall measured. ERA5 rainfall during that time was close to zero at



81.5° N, 16.75° W, while neighbouring grid cells have shown a similar amount of rainfall of 0.1 mm as the in situ measurements.

- 330 Apart from the first warm event the amount of precipitation in both datasets were similar, but the timing of precipitation events differed clearly. During PAMARCMiP, in situ measurements showed a snowfall event over several days, which is not present in ERA5 instead ERA5 showed about a week before the campaign snowfall. Field observations during PAMARCMiP confirmed strong snowfall events together with strong winds and snow drift.



- 335 **Figure 5: Atmospheric development from 15 February 2018 to end of PAMARCMiP campaign 08 April 2018. PAMARCMiP time is shown as the white and red area, whereby the red area is the time of the snowpit measurements. The shaded area around the orange line visualises minimum and maximum values simulated with four additional ERA5 grid cells nearest to Villum Research Station that are located on land. w.e. refers to water equivalent.**



3.2 Validation data

3.2.1 Snow depth

Overall ERA5-CTRL simulated the snow depth for the winter-centred years 2014/15, 2015/16 and 2016/17 in good agreement with the measurements (RMSD: 0.29 m) (Fig. 6). In these years, snow depth was within the co-location error of the ERA5 data until early spring. The snow depth measurements for PAMARCMiP showed distinctive differences in snow depth even over small distances. We measured snow depths from 60 to 117 cm with a standard deviation of 21.6 cm from the snow depth measurements during the detailed snowpits on 03 April 2018.

Melting started too early in the years 2015/16 and 2016/17 in ERA5-CTRL compared to the measurements (Fig. 6). Measured and simulated snow depth at the beginning and end of the snow season differed slightly, with the overall timing of the build-up of snow cover matching better than the precise timing of no snow cover. Date and amount of the maximum snow depth showed some moderate differences.

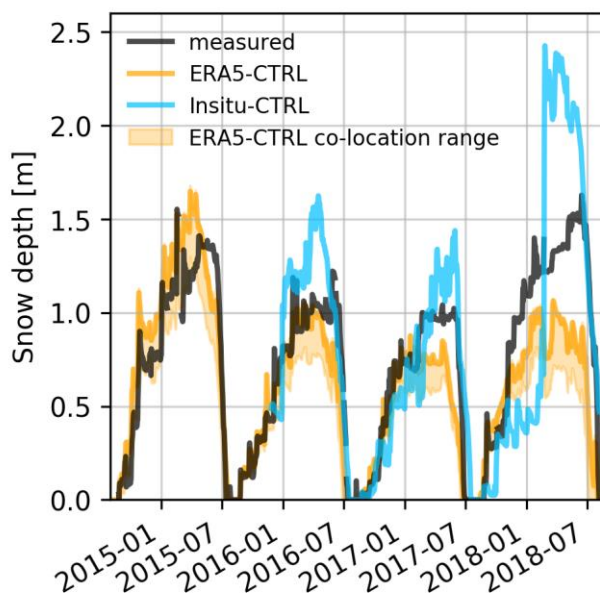
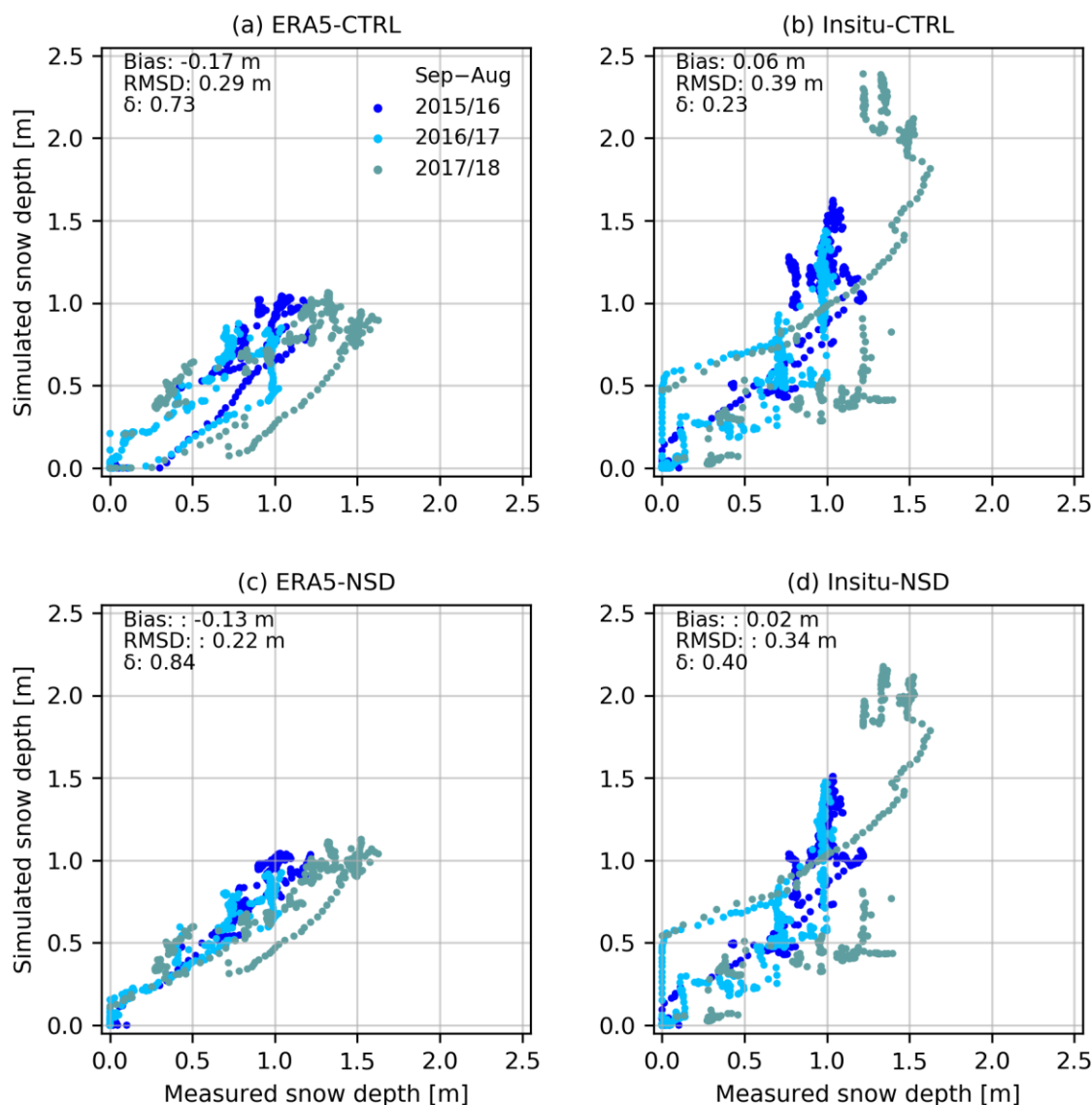


Figure 6: Snow depth at Villum Research Station from August 2014 to August 2018. Comparison of measured snow depth (black line) and simulated with ERA5-CTRL (orange line - closest ERA grid cell to Villum Research Station at 81.5° N, 16.75° W) and Insitu-CTRL (blue line – no data available before 27 November 2015). The orange shaded area visualises minimum and maximum snow depth of simulations at the four additional ERA5 grid cells nearest to Villum Research Station located on land and serve to illustrate the potential influence of the co-location error.

While the ERA5-CTRL onset of snow accumulation in 2017/18 was in good agreement with the observation, the simulation underestimated the snow depth from November 2017 onwards. From late February to mid March 2018, ERA5-CTRL overestimated the amount of melting, which further increased the difference between simulated and measured snow depth. The general onset of melting in 2018 occurred in the model already in May while the observed snow depth was still increasing.



360 Over the whole study period, the mean bias between ERA5-CTRL snow depth and the observation was only -0.17 m with a daily RMSD of moderate 0.29 m (Fig. 7a).



365 **Figure 7: Scatter diagram of measured and simulated daily snow depth between 27 November 2015 and 08 August 2018. The different colours visualise different years (a) and (b): ERA5-CTRL and Insitu-CTRL results with original parametrisation of new snow density V12 (c) and (d) ERA5-NSD and Insitu-NSD with the adapted new snow density parametrisation K21. Metrics displayed are the mean bias, root mean squared difference (RMSD) and explained variance δ .**

The snow depth simulated with Insitu-CTRL overestimated the snow depth in all three years. For this simulation the initial values (e.g. snow depth) was taken from the spin-up run with ERA5-CTRL forcing on 26 November 2015. Therefore, in 2015/16 Insitu-CTRL was certainly impacted by the initial values and difficult to evaluate, especially the simulated maximum snow depth. The end of the snow season for 2015/16 agreed well with the snow depth measurements (Fig. 6). For Insitu-CTRL

370



the onset of snow accumulation and snow depth for the year 2016/17 matched well until late spring. Later in the year the accumulation events were too strong leading to an overestimation of the snow depth. The end of the snow season occurred somewhat later than observed in 2017.

In 2017/18, Insitu-CTRL overestimated the maximum snow depth by almost a meter and showed a later increase in snow depth than measured and ERA5-CTRL. From late February to early March, there was a distinct increase in snow depth of about 1.5 m within a few days. Even if the mean bias between Insitu-CTRL and observed snow depth was low (0.06 m) and RMSD was 0.39 m over the whole study period, explained variance, which is the proportion of variability in the data explained by the model, was only 0.23 (Fig. 7b). For the same period ERA5-CTRL snow depth showed a much higher explained variance of 0.73.

As our sensitivity survey showed (Table 4), especially snowfall and specific humidity but also air temperature caused differences between simulated snow depth in Insitu-CTRL and ERA5-CTRL. The remaining forcing variables had clearly a lower impact on snow depth differences. The large response to the differences in specific humidity turned out to be an artefact of the linearisation. The experiment was rerun with a disturbance of $0.0002 \text{ kg kg}^{-1}$ and resulted in a difference in snow depth of 16.7 cm showing the limits of our approach – the sensitivity calculated for a disturbance of one tens of the standard deviation of the variability of the specific humidity was overestimated. Adding up the contributions of snowfall, specific humidity ($0.0002 \text{ kg kg}^{-1}$) and air temperature amounted to 0.29 m and compared well with the mean difference between Insitu-CTRL and ERA5-CTRL of 0.23 m.

Table 4: Results of sensitivity survey. CTRL refers to the control simulations described in Sect. 2.5. Mean difference between in situ and ERA5 2015 – 2018 refers to the atmospheric forcings while remaining columns refer to the simulations. DIR_SWdown: Direct incoming shortwave radiation, SCA_SWdown: Diffuse incoming shortwave radiation, LWdown: Incoming longwave radiation, Tair: Air temperature, PSurf: Surface air pressure, Qair: Specific humidity, Rainf: Rainfall and Snowf: Snowfall in water equivalent (w.e.).

	Mean difference in situ and ERA5 2015 - 2018	One-tens standard deviation ERA5	Snow depth difference ERA5-sens and ERA5-CTRL 2015 – 2018 [m]	Influence on snow depth difference Insitu-CTRL and ERA5-CTRL 2015 – 2018 [m]
DIR_SWdown [W m^{-2}]	-0.3	3.35	-0.007	0.001
SCA_SWdown [W m^{-2}]	-0.1	0.60	0.001	0
LWdown [W m^{-2}]	0	2.74	-0.01	0
Wind speed [m s^{-1}]	-0.2	0.17	-0.02	0.016
Tair [K]	1.0	0.42	-0.04	-0.091
PSurf [hPa]	0	0.80	0	0
Qair [kg kg^{-1}]	0.0002	4e-05	0.05	0.250
Qair 2e-04 [kg kg^{-1}]	0.0002	2e-04	0.17	0.167
Rainf [mm]	0.1	0.05	0	-0.001
Snowf [mm w.e.]	0.6	0.31	0.11	0.201

3.2.2 Snow density profiles

Comparisons between different approaches to receive density and SSA from SMP penetration force are shown in Fig. 8. While density calculated after Calonne et al. (2020) and King et al. (2020) showed some similarities, densities after Proksch et al.



(2015) were considerably higher in the upper part of the profiles and generally more variable expressed in larger standard deviation ranges (Fig. 8 shaded areas). SSA after Calonne et al. (2020) differed strongly from Proksch et al. (2015) and is clearly higher and more variable.

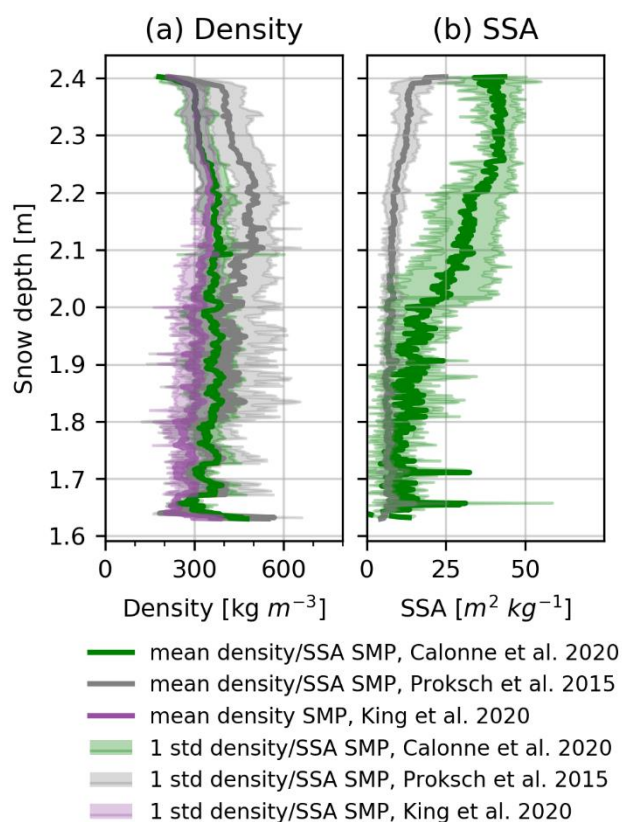


Figure 8: Comparison of SnowMicroPen (SMP) parametrisations of Calonne et al. (2020), Proksch et al. (2015) and King et al. (2020) (only density) to obtain (a) snow density and (b) specific surface area (SSA) from penetration force measured on 23 March 2018.

We compared the snow density profiles obtained from a SMP after Calonne et al. (2020) on 23 March 2018 with the simulations (Fig. 9a, b). Additionally, we compared the simulations to a density profile obtained with a density cutter on 03 April 2018 (Figure 10a, b). Overall, simulated and measured density profiles showed a poor agreement for the CTRL simulations. Simulated snow densities, both in ERA-CTRL and Insitu-CTRL were much lower than measured with the SMP or with the density cutter. This was especially true for the upper part of the profile.

Density variations with depth within the simulated snowpack were mostly small. Simulated snow densities showed a clear densification with depth and did not capture the snow density decrease from 388 kg m^{-3} to 270 kg m^{-3} measured with the density cutter in the lower part of the snowpack (e.g. below 0.3 normalised snow depth, Fig. 10a). SMP measurements showed a pronounced increase in the density from 180 kg m^{-3} to 300 kg m^{-3} over a few centimetres below the snow surface, which



density cutter measurements could not resolve. Both simulations were not able to capture this density increase near the surface (Fig. 9a, b).

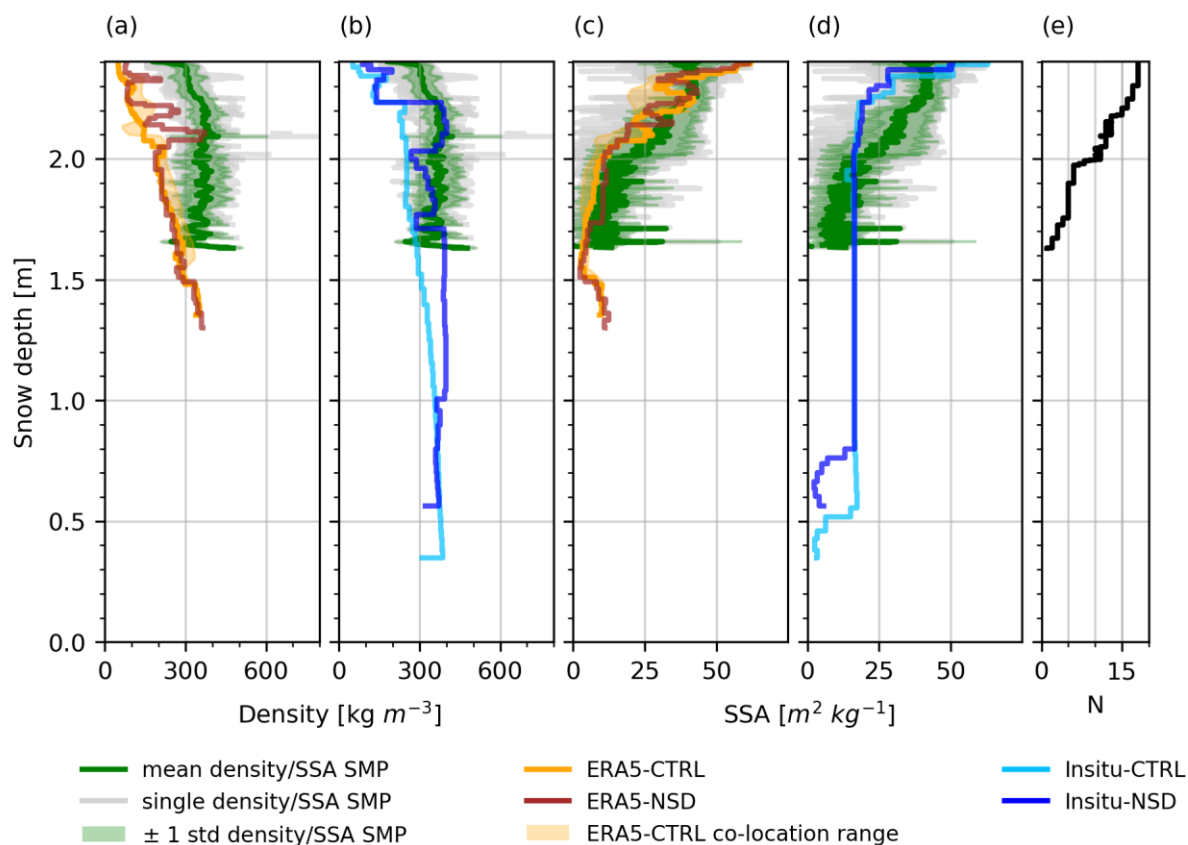


Figure 9: Simulated and measured snow density and specific surface area (SSA) on 23 March 2018. Measured density and SSA are derived after Calonne et al. (2020) from the SnowMicroPen (SMP). (a) and (b) display snow density, (c) and (d) SSA and (e) the sampling frequency. “CTRL” use the new snow density parametrisation V12 and “NSD” use K21. Snow depth baseline is the maximum snow depth during PAMARCMiP campaign of all measurements and simulations (2.4 m). Single density/SSA SMP shows measured single SMP profiles. The meaning of the colours are expressed in the legend.

Density in Insitu-CTRL was higher than in ERA5-CTRL on 23 March 2018 and 03 April 2018. In Fig. 10b thick snow layer of recent snowfall was visible at the top of the profile (1–0.85 normalised snow depth) in Insitu-CTRL. Also, density in ERA5-CTRL indicated some recent snowfall but less pronounced (1–0.9 normalised snow depth).

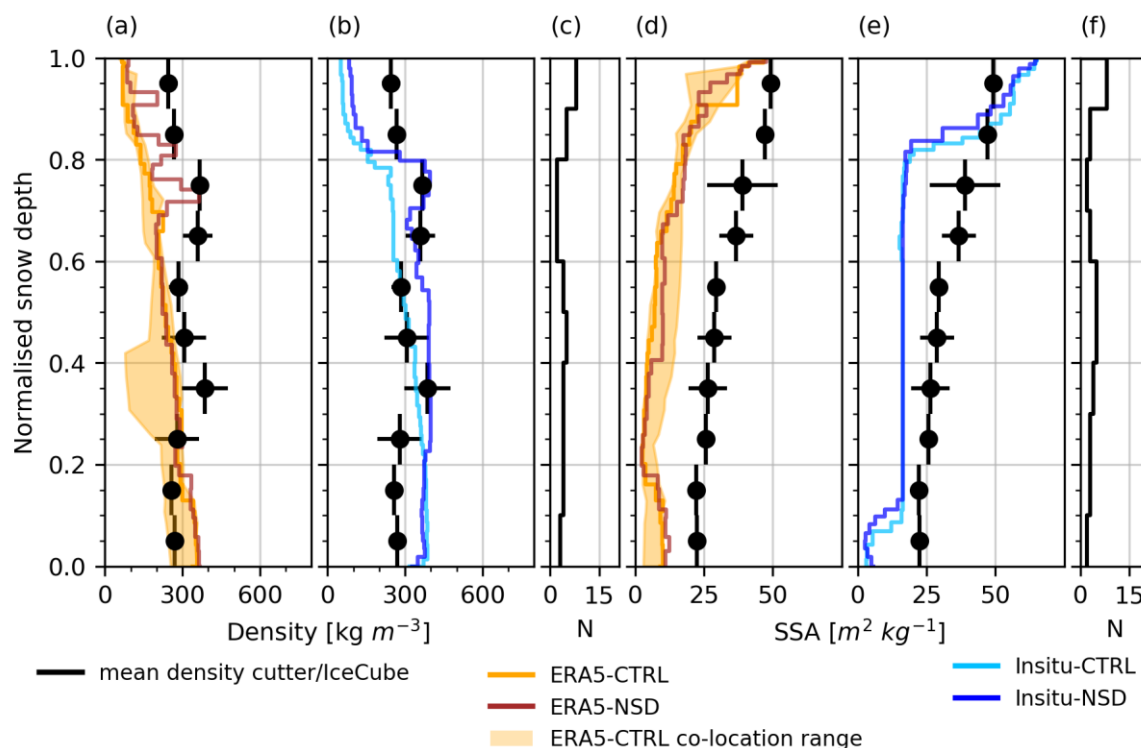


Figure 10: Simulated and measured snow density from density cutter and specific surface area (SSA) from IceCube on 04 April 2018. (a) and (b) display snow density, (d) and (e) SSA and (c) and (f) the sampling frequency. “CTRL” use the new snow density parametrisation V12 and “NSD” use K21. The meaning of the colours are expressed in the legend.

3.2.3 SSA profiles

Overall, SSA measured by the SMP and simulated were in good agreement when the sample variability of the measurements is taken into account (the simulated SSA were within the range spanned by ± 1 standard deviation of the sampling variability).
 430 SSA in ERA5-CTRL was much more variable on 23 March 2018 than in Insitu-CTRL (Fig. 9c, d). SSA in ERA5-CTRL showed three peaks while SSA in Insitu-CTRL is similar to ERA5-CTRL but showed less variability. Measured SSA with the SMP showed a huge standard deviation, which led to some match with simulated SSA even if both simulated profiles differed by about $10 \text{ m}^2 \text{kg}^{-1}$ in average.

The vertical pattern of the SSA profiles of both simulations were similar to observations taken with the IceCube on 03 April 2018 (Fig. 10). All profiles showed a decrease in SSA from the surface towards the middle part of the snow continued by an almost constant course to greater depth. However, amplitudes of the decrease and the height of SSA differed considerably. ERA5-CTRL on 03 April 2018 started at the surface with a reliable SSA of $47 \text{ m}^2 \text{kg}^{-1}$ but decreased earlier and stronger than the measurements with depth (Fig. 10d). Therefore, ERA5-CTRL underestimated SSA over the whole snow profile and showed mostly values below Insitu-CTRL. SSA in ERA5-CTRL decreased from the top of the snowpack until 0.6 m, followed



440 by a more or less constant middle part with SSA lower than $10 \text{ m}^2 \text{ kg}^{-1}$. SSA increased in the lower part of the profile until the ground, which contradicts the measurements. SSA in In-situ-CTRL (Fig. 10e) showed an overestimation of surface SSA of about $15 \text{ m}^2 \text{ kg}^{-1}$. Insitu-CTRL SSA decreased stronger than measured SSA before it became stable from 0.8 to 0.1 normalised snow depth while measured SSA showed a slight decrease over the whole profile with higher SSA than Insitu-CTRL. Overall, ERA5-CTRL and Insitu-CTRL could capture the gross profile of measured SSA. ERA5-CTRL started with more
 445 reliable surface SSA than Insitu-CTRL. However, both simulations failed to reproduce the details in the measured SSA profiles. Moreover, the SSA decreasing rates from top to bottom of the profiles were different for simulations and measurements.

3.2.4 Impacts of the new snow density parametrisation

With the introduced new snow density parametrisation K21, we could reduce mean bias and RMSD of snow depth in ERA5-
 450 NSD by 0.04 m and 0.07 m, respectively, for the simulated period 2015 to 2018 (Fig. 7c). Furthermore, the explained variance increased by 0.11 to 0.84. The Insitu-NSD's snow depth mean bias and RMSD could be improved for snow depth by 0.04 m and 0.05 m, respectively. The explained variance increased by 0.17 to 0.40 (Fig. 7d).

Figure 11 visualises the measured and simulated snow depth time series for CTRL and NSD simulations. ERA5-NSD's snow depths were slightly higher towards the end of the snow season than ERA5-CTRL's (Fig. 11a). Insitu-NSD showed clearly
 455 lower snow depths than Insitu-CTRL for 2015/16 and 2017/18 (Fig. 11b).

Applying K21, we obtained more reliable density simulations than using the original parametrisation V12. The simulated snow densities showed a much higher variability with several distinct density peaks, which were also visible in the SMP profiles and the density cutter profiles (Fig. 9a, b and Fig. 10a, b). The densities with K21 were also considerably higher than with V12. Furthermore, the snow density not only increased with depth, but also showed more pronounced variability.

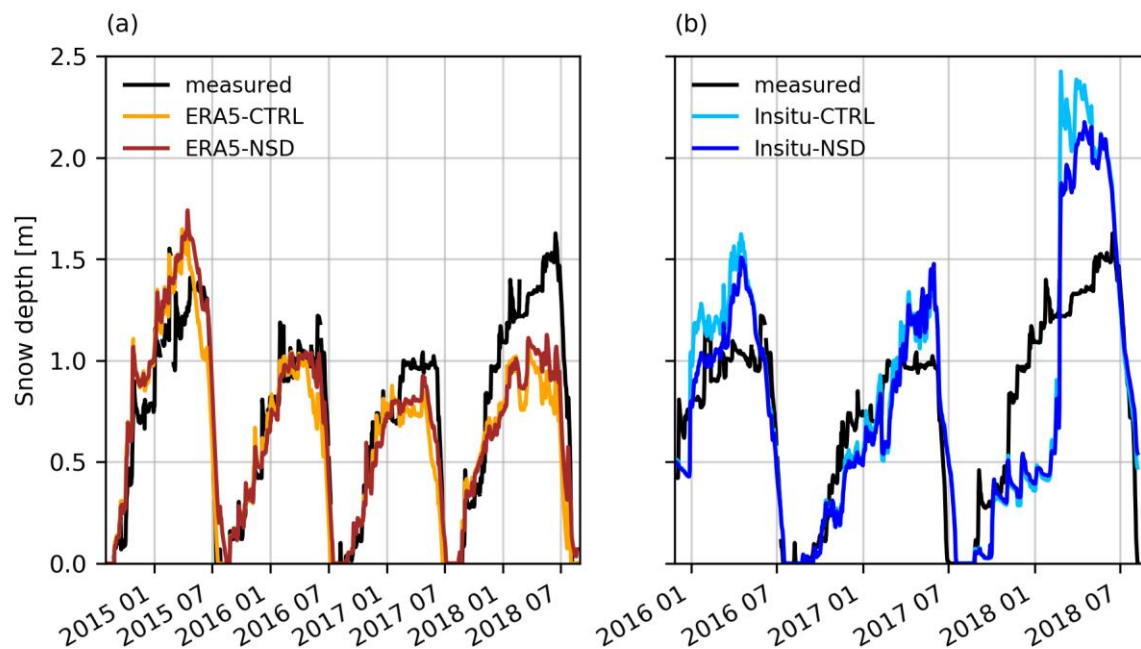


Figure 11: Comparison of measured and simulated snow depth with the new snow density parametrisation V12 (CTRL) and the introduced K21 parametrisation (NSD). For (a) ERA5 simulations from August 2014 to August 2018 and (b) in situ simulations from 27 November 2015 to August 2018.

With K21, we could occasionally reach the sample variability ranges of the measurements. However, it was still not possible to simulate the sharp density increase near the snow surface observed with the SMP. Also, the model could not capture the decrease in snow density towards the ground as measured with the density cutter. The underestimation of the density in the uppermost layers and the overestimation of the basal layers remained.

K21 affected the simulated SSA to a smaller extent than the snow density. The overall SSA profile of ERA5-NSD was similar to ERA5-CTRL on 23 March 2018 (Fig. 9c, d). SSA in Insitu-NSD changed mainly in the upper and in the lower part of the profile while the middle part remained: After the decrease of SSA to $20 \text{ m}^2 \text{ kg}^{-1}$, SSA remained constant as in Insitu-CTRL, but increased slightly before the decrease at the lower part of the profile. Changes due to K21 on 03 April 2018 compared to SSA obtained with the IceCube were similar to SSA obtained by the SMP on 23 March 2018 (Fig. 10c, d).

4 Discussion

4.1 Forcing data

One of the advantages of ERA5 is its physical consistency and completeness of time series, which is not the case with the in situ measurements. However, the reanalysis is only able to resolve processes, which are within the scales of motion of the model resolution or even larger (Minola et al., 2020). Precipitation on a kilometre scale can already vary significantly (Betts



et al., 2019). Therefore, ERA5 cannot resolve e.g. local precipitation events also visible in the atmospheric data during PAMARCMiP where ERA5 underestimates precipitation during the warm event in the second half of February 2018.

480 Atmospheric variables measured at Villum Research Station are point measurements representing local conditions. ERA5 on the other hand represents mean values over a whole grid cell. Due to the relatively coarse resolution of ERA5, the relief is much smoother than in reality. This causes altitudinal differences and leads to different values e.g. in surface air pressure than observed. After correcting for this altitudinal differences ERA5 air pressure agrees well with measurements, which is in line with the findings of Delhasse et al. (2020a).

485 We find a good correspondence between measured and ERA5 air temperatures, shortwave and longwave radiation with only minor differences in agreement with other studies (Betts et al., 2019; Wang et al., 2019; Delhasse et al., 2020a). Differences in observed and ERA5 surface air temperature can also result from the elevation difference between Villum Research Station and the ERA5 grid cell. In our study, the use of longwave radiation from ERA5 instead of observations for the in situ forcing enabled us to circumvent measurement errors caused by a tilted sensor.

490 Differences in local topography due to the relative coarse resolution of ERA5 also affect wind speed and wind direction (Delhasse et al., 2020a). Higher obstacles to the southeast from Villum Research Station, not resolved correctly by ERA5, can alternate and influence wind direction and wind speed. In addition, the vertical interpolation from higher levels with negligible influence of its underlying terrain causes differences in wind speed and wind direction between the reanalysis and in situ measurements. This can be problematic in terms of snow modelling, as wind is an important variable to correctly simulate

495 snow density due to wind compaction, enhanced sublimation and wind redistribution at higher wind speeds.

In our study, ERA5 overestimates mean wind speed over the whole study period while Betts et al. (2019) found an underestimation for the Canadian Prairies. Delhasse et al. (2020a) identified an underestimation over stations located mainly in the ablation area of the Greenland Ice Sheet but mostly overestimation for stations located mainly in the accumulation area (Delhasse et al., 2020b). We identify a higher wind speed underestimation for higher ERA5 wind speeds in agreement with

500 Betts et al. (2019) and Delhasse et al. (2020a). Betts et al. (2019) identified an quasi-linearly increasing underestimation of wind speed for ERA5 while Delhasse et al. (2020a) described an enhanced underestimation for wind speeds higher than 3 m s^{-1} . Our analyses of the wind direction show strong differences between reanalysis and in situ data, although our simulations are not impacted because of no aspect ratio prescribed. However, the huge difference between measured wind direction and reanalysis might be of interest for others using ERA5. Especially when it comes e.g. to modelling of snow redistribution by

505 snowdrift, wind direction plays an important role and has to be handled with care.

Crocus requires a separation in liquid and solid precipitation. We used the approach after Jennings et al. (2018) and defined all precipitation as solid for surface air temperature lower than 1°C . Such a simple approach does not represent the reality as the phase transition spread out over about -2°C and $+4^\circ\text{C}$ over land area (Dai, 2008). As snowfall is one of the major factors determining simulated snow depth and other snow properties, the separation in liquid and solid precipitation adds to the

510 uncertainty. Another source of uncertainty is the conversion from relative humidity and dew point into specific humidity using



surface air pressure and air temperature. Due to different available variables (ERA5: dew point, in situ: relative humidity), we had to choose different approaches to obtain specific humidity.

Furthermore, large measurement gaps in total precipitation (35.2 % missing values) are problematic. We introduce an underestimation of precipitation by setting these gaps to zero precipitation, which leads to underestimation of in situ precipitation. However, in situ simulations clearly overestimate the snow depth although missing precipitation values are set to zero, i.e. our simulation suggest that the in situ precipitation is not consistent to the measured snow depth. False precipitation measurements can be caused by snowdrift, which is falsely detected as precipitation.

ERA5 is able to catch the heat waves and strong winds in the second half of February 2018. Most variables match well during this period apart from precipitation and some minor deviations in wind direction and hourly wind speed during peak times, where hourly ERA5 wind speed underestimates. In agreement with Delhasse et al. (2020a), Betts et al. (2019) and Wang et al. (2019) and despite differences due to topographic and vertical resolution of ERA5, atmospheric variables used in Crocus agree well with in situ measurements except during local precipitation events.

4.2 Validation data

4.2.1 Snow depth

Snow depth varies considerably even on small spatial scales. With the SA50A-sensor at Villum Research Station, we can only measure local snow depth. On 03 April 2018, when the detailed snow pit measurements were performed, snow depth measurements varied in the vicinity of Villum Research Station between 60 and 117 cm with a standard deviation of 21.6 cm. This might be caused by several small depressions and bumps that influenced local snow depth. Also other studies found differences of 0.45 m to more than 1 m in snow accumulation over the course of a year within a radius of several kilometres (Domine et al., 2016a; Pedersen et al., 2016). Reasons for this include snow redistribution by wind, microtopographic relief and vegetation (Barrere et al., 2017; Liston and Sturm, 2002).

Surprisingly ERA5 simulated snow depth clearly outperforms in situ forced snow depth. Taking into account the considerable spatial snow depth variability, simulated ERA5 snow depth, which represents a mean of the grid cell, agrees unexpectedly well with the point measurements at Villum Research Station. The simulated in situ snow depth shows larger deviations from the measured snow depth than the ERA5 simulation. The simulated in situ snow depth considerably overestimates. We did not expect that result as atmospheric forcing is measured nearby and we treated missing precipitation measurements (~35.2 % missing values) as no precipitation. Hence, we expected an underestimation of snow depth rather than an overestimation. Reasons for the overestimation could be failures of the TPS-3100-sensor of Villum Research Station (precipitation data is not quality controlled) or massive influence of snow redistribution due to wind drift.

We can show that Crocus is able to simulate reliable snow depth evolutions for the Arctic when uncertainties of the atmospheric forcing are negligible. Other studies have come to the same conclusion when adjusting the model or the forcing data (Luijting et al., 2018; Jacobi et al., 2010; Sauter and Obleitner, 2015; Barrere et al., 2017). Nevertheless, Luijting et al. (2018) found



accumulated over- and underestimations of snow depth of about 1 m over a season. This finding confirms our observations where e.g. ERA5 considerably underestimates snow accumulation during the warm air intrusion in spring 2018 and other precipitation events, which accumulates to a strong underestimated snow depth throughout the season. In our study, also deviations in simulated and measured snow densities e.g. due to an underestimation of new snow densities, lead to differences in snow depth between simulations and measurements. This correspondence with findings from Sauter and Obleitner (2015) and Essery et al. (2016).

We find highest impacts of simulated snow depth on uncertainties in snowfall, specific humidity and air temperature. Sauter and Obleitner (2015) showed that uncertainties in forcing can lead to more than 3 m deviation in snow depth after one year. This again highlights how problematic biases due to missing data, snowdrift and riming on instruments and measurement uncertainties in the measured data or ERA5 data are.

Furthermore, snow redistribution due to strong winds is not parametrised in the model and could be therefore another reason for deviations between observed and simulated snow depth. In the Arctic, snow redistribution is very important. Therefore, adding this process to Crocus could lead to substantial improvements in simulated snow depth (Barrere et al., 2017; Luijting et al., 2018; Libois et al., 2014). The influence on density and increased sublimation due to snowdrift, already parametrised in the model, lead to distinctively lower snow depths in our simulations. However, the quality of the parametrisation of the increased sublimation during snowdrift requires more detailed consideration in future studies.

Crocus reproduces well the observed onset of snow accumulation in our study, while melting starts earlier and is faster than observed. The discrepancies in the timing and development of thawing are a widely observed problem in the application of Crocus in the Arctic (Barrere et al., 2017; Essery et al., 2016; Domine et al., 2019; Luijting et al., 2018; Jacobi et al., 2010). Reasons for this could be a higher simulated thermal conductivity of the basal snow layer and a lower simulated thermal conductivity of the near-surface layers (Barrere et al., 2017; Domine et al., 2019) as well as the lack of parametrisation of snow redistribution by wind (Luijting et al., 2018).

4.2.2 Snow density and SSA profiles

A typical Arctic snow profile shows a basal depth hoar layer with low density ($150\text{--}200\text{ kg m}^{-3}$) and high density at the top wind slab snow layers (exceeding 400 kg m^{-3}) (Barrere et al., 2017). In our SMP measurements, a density peak is visible near the surface. In the density cutter measurements we can observe a density decrease towards the basal layers. In addition, observations during fieldwork also indicate a bottom depth hoar layer in our profiles. However, due to the lack of detailed determination of stratigraphy, we cannot fully confirm the typical snow stratification from our observations.

While Essery et al. (2016) found a strong correlation between simulated and observed snow density profiles ($r=0.74$), we find considerable differences in both CTRL simulations. We see a constant increase in density with depth. This is typical for Alpine snow, where dense basal layers are common (Domine et al., 2019). Simulations overestimate density for near surface snow layers and underestimate density for basal snow layers. This corresponds with results from other studies (Gascon et al., 2014; Jacobi et al., 2010; Domine et al., 2019; Barrere et al., 2017). Our results show clearly that an important process



determining the snow stratigraphy in the Arctic is missing in Crocus. Barrere et al. (2017) and Jacobi et al. (2010) considered the main reason for the inverted density profiles in the lack of a parametrisation of upward water vapour transport due to strong temperature gradients occurring in the Arctic. Several other model deficiencies can also lead to an incorrect simulation of the Arctic snow profile (Gascon et al., 2014; Domine et al., 2016b; Barrere et al., 2017).

580 We found an underestimation of new snow density with Crocus, which confirms the results from other studies in the Arctic (Sauter and Oblaitner, 2015; Essery et al., 2016; Lefebvre et al., 2005). In the new snow density parametrisation currently used in Crocus, new snow density is set to 50 kg m^{-3} for temperatures below -30°C , which are common in Arctic winter, and a linear relationship between temperature and density is applied (Vionnet et al., 2012). In contrast, Meister (1985) found increasing new snow densities for temperatures below -15°C as we considered with the introduced new snow density parametrisation
 585 K21. Braking through wind impacts and crystallization at low temperatures are reasons for a higher new snow density in the Arctic than in the warmer and more sheltered European Alps (Jordan et al., 1999). Applying K21 results in a denser new snow density in our study and thus higher maximum densities for the uppermost snow layers than with the original formulation. With an for the Arctic adapted new snow density parametrisation we find that Crocus is able to reproduce the gross density profile and stratification for an Arctic snowpack in line with Sauter and Oblaitner (2015).

590 A realistic simulation of snow density is crucial. Crocus uses a function of density to parametrise important snow properties like SSA or thermal conductivity (Vionnet et al., 2012; Carmagnola et al., 2014). Incorrect simulated snow densities lead to erroneous thermal conductivities, which serve as input for the calculation of the temperature gradient. Therefore, the simulated metamorphism is erroneous (Domine et al., 2019). As density is a key variable influencing other important variables in Crocus, we assume that differences in simulated and measured densities can partly explain differences in simulated and measured SSA.
 595 SSA is parameterised in Crocus as an inverse function of the optimal diameter (Carmagnola et al., 2014). Therefore, e.g. an inverted stratification of snow density leads to a lower SSA and thus to a lower albedo simulated with Crocus (Domine et al., 2019). In reality, differences in SSA of snow profiles can also result from variations in snow depth, density and temperature (Jacobi et al., 2010; Carmagnola et al., 2014). SSA further depends on wind speed and temperature gradient (Domine et al., 2019; Carmagnola et al., 2014). Furthermore, uncertainties in the forcing data can lead to erroneous simulated densities and
 600 SSA as visible in deviations in ERA5-CTRL and Insitu-CTRL SSA on 03 April 2018 (Fig. 10). Different timing of a precipitation event in measurements and ERA5 causes these differences. In agreement with Carmagnola et al. (2014) we find discrepancies between simulations of SSA and IceCube measurements. Strong temperature gradients in the Arctic not captured by Crocus (Domine et al., 2019) could partly explain differences in our simulated and measured SSA profiles.

Our density and SSA measurements have weaknesses in capturing the whole spatial variability around Villum Research Station
 605 due to limited measurement profiles. However, examined profiles were carried out in representative areas of the vicinity of Villum Research Station. Due to many thin ice lenses within the snowpack, the SMP could not penetrate through the entire snowpack. Therefore, the results give just a reasonable approximation for the surface layer.

Another uncertainty of SMP measurements is the calculation of snow density and SSA from penetration force. We applied three parametrisations to our data, with considerably different results (Fig. 9). For the development of the parametrisation,



610 Proksch et al. (2015) used data from the European Alps and the Arctic, while measurements for the parametrisation after
 Calonne et al. (2020) were from the Swiss Alps and therefore for warm snow. However, Calonne et al. (2020) developed the
 parametrisation for the SMP Version 4 we used, while the parametrisation after Proksch et al. (2015) was developed for SMP
 Version 2 (Calonne et al., 2020). King et al. (2020) found large discrepancies between measured density with a density cutter
 and SMP after Proksch et al. (2015) for snow on Arctic sea ice. Parametrisation for SSA after Proksch et al. (2015) was
 615 developed using the precise MicroCT while Calonne et al. (2020) used measurements from the IceCube. We found that
 densities for Calonne et al. (2020) and King et al. (2020), whose parametrisation is for Arctic snow on sea ice with the SMP
 Version 4, differ only slightly. Simulated density is closest to results after King et al. (2020) and Calonne et al. (2020) and
 especially underestimated compared to densities after Proksch et al. (2015). Simulated SSA agrees better with results after
 Calonne et al. (2020) and is far off results after Proksch et al. (2015). Nevertheless, a reliable comparison between our
 620 simulations and the density and SSA derived from SMP is not possible due to uncertainties in the algorithms used to derive
 these quantities.

Taken into account uncertainties due to the high spatial variability of snow density and SSA visible in the variety of the
 measurements, we observe a fair agreement of the ERA5-NSD profiles with the measurements. However, we cannot simulate
 the strong increase in the measured density in the upper layers. In addition, underestimations of snow density in the upper
 625 layers and overestimations in the lower layers remain. We assume that the main reason for this is the lack of parametrisation
 of the vertical water vapour transport and the resulting mass transport from lower to upper snow layers. With further adaptations
 of Crocus and inclusion of this missing process relevant for the Arctic, we expect better results.

5 Conclusion

Working with snow in the Arctic is challenging due to limited temporal and spatial availability of measured snow data. Detailed
 630 snow models can help to overcome this problem and can assist to interpret the measurements but require carefully prepared
 forcing data to ensure a good quality of simulated snow data. Using the snow model Crocus, we can show that already small
 deviations in solid precipitation, specific humidity and air temperature lead to considerable differences in simulated snow
 depth.

In situ atmospheric measurements in the Arctic are rare, incomplete, and have to cope with difficult measurement conditions
 635 such as riming on the instruments and strong winds, while models need complete time series to drive them. Our study
 demonstrates that the reanalysis ERA5, except for precipitation, wind speed, and wind direction, agrees well with atmospheric
 measurements at Villum Research Station in northeast Greenland between October 2014 and August 2018. ERA5 is also
 physically consistent being an output of a numerical atmospheric model, which does not apply for the observations, explaining
 partly a higher agreement of simulated and measured snow depth under ERA5 forcing than with in situ forcing, a result not
 640 has been expected.



Due to the relatively coarse resolution of ERA5, topography is not resolved in detail. Presumably for that reason, ERA5 cannot reproduce small-scale local precipitation events. Observed and reanalysis precipitation also do not match in time. Differences in topography influence wind direction and wind speed, thus ERA5 underestimates higher wind speeds in particular. Due to differences in elevation between the grid cell and the observation site, there are differences in air temperature and surface air pressure.

Overall, our study shows that ERA5 is capable to replace in situ measurements to force snow models where observations are limited, considering the limitations of in situ data and the reanalysis. Our study site is located in an area influenced by orography. We expect higher agreement of ERA5 and observations for flat areas as widely common in the Arctic such as sea ice. ERA5 will be a useful dataset for future studies in the Arctic, which need complete time series of meteorological data. Our first question raised in the introduction if ERA5 data can be used as a surrogate for missing in situ forcing data can be unambiguously affirmed.

Concerning our second research question, whether the Alpine snow model Crocus can reliably simulate snow depth development as well as snow density and SSA profiles, we cannot give a conclusive answer as Crocus can simulate the rough evolution of snow depth, but not of SSA and snow density of an Arctic snowpack. Thereby the ERA5 simulations outperforms in situ simulations. Differences between Alpine and Arctic atmospheric conditions and thus snow properties and processes can explain the deviations between observations and simulations in the Arctic. Crocus strongly underestimates new snow density, leading to an underestimation of snow density over the entire profile. In our study, we introduce a different new snow density parametrisation that results in more representative snow densities for Arctic snow profiles than with the original parametrisation. Using our new snow density parametrisation, Crocus still underestimates snow density in the upper layers and overestimate snow density in the basal layers. We attribute this to a lack of parametrisation of important processes in the Arctic such as vertical water vapour transport and snow redistribution by strong winds.

Our study shows that Crocus has great potential for simulating snow conditions in the Arctic. The model can contribute to complement temporally and spatially limited observed snow depth measurements through representative simulations. Simulated and observed snow densities and SSA show deviations of which the user needs to be aware. Having that in mind, Crocus can give added value to the evolution and the range of the prevailing density and SSA. This is a clear improvement over the otherwise frequent use of fixed density values for all layers and values from climatologies for e.g. ice-ocean models. We hope this manuscript is a step forward to achieve these goals.

Author contribution. DK carried out the analysis, performed the model simulations, drafted the manuscript and prepared the figures. FK helped with fruitful discussions of the analysis and designed the methodology of the sensitivity survey. All authors contributed to the editing of the manuscript. AH helped with the observational design of the study. FK and MD assisted with the numerical design. AH was leading the PAMARCMiP campaign.



Acknowledgments

The PAMARCMiP campaign was funded by the Deutsche Forschungsgemeinschaft (DFG, German Research Foundation) – project ID 268020496 – TRR 172, within the Transregional Collaboration Research Center ‘Arctic Amplification: Climate Relative Atmospheric and Surface Processes, and Feedback Mechanisms (AC)3. We thank Marco Zanatta for the snow sampling during the campaign and Villum Research Station for general support. Special thanks go to Keld Mortensen and Andreas Massling for providing observational meteorological data. The authors acknowledge the cooperation and the productive scientific discussion with Christian Haas, Stefanie Arndt, Marco Zanatta and Olaf Eisen. CNRM/CEN is part of Labex OSUG@2020 (ANR-10-LABX-0056). M.D. has received funding from the European Research Council (ERC) under 20 the European Union’s Horizon 2020 research and innovation programme (grant agreement No 949516, IVORI).

Data availability: The snow properties data as well as the results of the model simulations are intended to be published on PANGAEA. ERA5 data are publically available from the Climate Data Store (<https://cds.climate.copernicus.eu/cdsapp#!/dataset/reanalysis-era5-single-levels?tab=form> or via Climate Data Store API).

Competing interests. MD is a member of the editorial board of the The Cryosphere. All other authors declare that they have no conflict of interest.

References

- A2 Photonic Sensors: IceCube: Innovative optical system for measurement of the specific surface area (SSA) of snow, available at: http://www.a2photonicsensors.com/medias/A2PS_IceCube_EN.pdf, 2016.
- Albergel, C., Dutra, E., Munier, S., Calvet, J.-C., Munoz-Sabater, J., Rosnay, P. de, and Balsamo, G.: ERA-5 and ERA-Interim driven ISBA land surface model simulations: which one performs better?, *Hydrol. Earth Syst. Sci.*, 22, 3515–3532, <https://doi.org/10.5194/HESS-22-3515-2018>, 2018.
- Anderson, E. A.: A point energy and mass balance model of a snow cover, NOAA technical report, NWS 19, U.S. Dept. of Commerce, National Oceanic and Atmospheric Administration, National Weather Service, Office of Hydrology, Silver Spring, Md., xviii, 150 p, 1976.
- ASIAQ: Weather station at Station Nord Technical Documentation. Obtained by personal contact with Villum Research Station., 2014.
- Barrere, M., Domine, F., Decharme, B., Morin, S., Vionnet, V., and Lafaysse, M.: Evaluating the performance of coupled snow–soil models in SURFEXv8 to simulate the permafrost thermal regime at a high Arctic site, *Geosci. Model Dev.*, 10, 3461–3479, <https://doi.org/10.5194/gmd-10-3461-2017>, 2017.
- Bartelt, P. and Lehning, M.: A physical SNOWPACK model for the Swiss avalanche warning, *Cold Regions Science and Technology*, 35, 123–145, [https://doi.org/10.1016/S0165-232X\(02\)00074-5](https://doi.org/10.1016/S0165-232X(02)00074-5), 2002.



- 710 Betts, A. K., Chan, D. Z., and Desjardins, R. L.: Near-Surface Biases in ERA5 Over the Canadian Prairies, *Front. Environ. Sci.*, 7, 129, <https://doi.org/10.3389/fenvs.2019.00129>, 2019.
- Boelman, N. T., Liston, G. E., Gurarie, E., Meddens, A. J. H., Mahoney, P. J., Kirchner, P. B., Bohrer, G., Brinkman, T. J., Cosgrove, C. L., Eitel, J. U. H., Hebblewhite, M., Kimball, J. S., LaPoint, S., Nolin, A. W., Pedersen, S. H., Prugh, L.,
 710 R., Reinking, A. K., and Vierling, L. A.: Integrating snow science and wildlife ecology in Arctic-boreal North America, *Environ. Res. Lett.*, 14, 10401, <https://doi.org/10.1088/1748-9326/aaec1>, 2019.
- Boone, A., Masson, V., Meyers, T., and Noilhan, J.: The Influence of the Inclusion of Soil Freezing on Simulations by a Soil–Vegetation–Atmosphere Transfer Scheme, *Journal of Applied Meteorology and Climatology*, 39, 1544–1569, [https://doi.org/10.1175/1520-0450\(2000\)039<1544:TIOTIO>2.0.CO;2](https://doi.org/10.1175/1520-0450(2000)039<1544:TIOTIO>2.0.CO;2), 2000.
- 715 Box, J. E., Fettweis, X., Stroeve, J. C., Tedesco, M., Hall, D. K., and Steffen, K.: Greenland ice sheet albedo feedback: thermodynamics and atmospheric drivers, *The Cryosphere*, 6, 821–839, <https://doi.org/10.5194/TC-6-821-2012>, 2012.
- Brun, E., David, P., Sudul, M., and Brunot, G.: A numerical model to simulate snow-cover stratigraphy for operational avalanche forecasting, *J. Glaciol.*, 38, 13–22, <https://doi.org/10.3189/S0022143000009552>, 1992.
- 720 Callaghan, T. V., Johansson, M., Brown, R. D., Groisman, P. Y., Labba, N., Radionov, V., Bradley, R. S., Blangy, S., Bulygina, O. N., Christensen, T. R., Colman, J. E., Essery, R. L. H., Forbes, B. C., Forchhammer, M. C., Golubev, V. N., Honrath, R. E., Juday, G. P., Meshcherskaya, A. V., Phoenix, G. K., Pomeroy, J., Rautio, A., Robinson, D. A., Schmidt, N. M., Serreze, M. C., Shevchenko, V. P., Shiklomanov, A. I., Shmakin, A. B., Sköld, P., Sturm, M., Woo, M., and Wood, E. F.: Multiple Effects of Changes in Arctic Snow Cover, *AMBIO*, 40, 32–45, <https://doi.org/10.1007/S13280-011-0213-X>, 2011.
- 725 Calonne, N., Richter, B., Löwe, H., Cetti, C., Schure, J. ter, van Herwijnen, A., Fierz, C., Jaggi, M., and Schneebeli, M.: The RHOSSA campaign: multi-resolution monitoring of the seasonal evolution of the structure and mechanical stability of an alpine snowpack, *The Cryosphere*, 14, 1829–1848, <https://doi.org/10.5194/tc-14-1829-2020>, 2020.
- Carmagnola, C. M., Morin, S., Lafaysse, M., Domine, F., Lesaffre, B., Lejeune, Y., Picard, G., and Arnaud, L.: Implementation and evaluation of prognostic representations of the optical diameter of snow in the SURFEX/ISBA-Crocus detailed snowpack model, *The Cryosphere*, 8, 417–437, <https://doi.org/10.5194/tc-8-417-2014>, 2014.
- 730 Dai, A.: Temperature and pressure dependence of the rain-snow phase transition over land and ocean, *Geophys. Res. Lett.*, 35, <https://doi.org/10.1029/2008GL033295>, 2008.
- Delhasse, A., Kittel, C., Amory, C., Hofer, S., van As, D., S. Fausto, R., and Fettweis, X.: Brief communication: Evaluation of the near-surface climate in ERA5 over the Greenland Ice Sheet, *The Cryosphere*, 14, 957–965, <https://doi.org/10.5194/tc-14-957-2020>, 2020a.
- 735 Delhasse, A., Kittel, C., Amory, C., Hofer, S., van As, D., S. Fausto, R., and Fettweis, X.: Supplement of Brief communication: Evaluation of the near-surface climate in ERA5 over the Greenland Ice Sheet, *The Cryosphere*, 14, <https://doi.org/10.5194/tc-14-957-2020-supplement>, 2020b.



- Domine, F., Picard, G., Morin, S., Barrere, M., Madore, J.-B., and Langlois, A.: Major Issues in Simulating Some Arctic
 740 Snowpack Properties Using Current Detailed Snow Physics Models: Consequences for the Thermal Regime and Water
 Budget of Permafrost, *J. Adv. Model. Earth Syst.*, 11, 34–44, <https://doi.org/10.1029/2018MS001445>, 2019.
- Domine, F., Gauthier, G., Vionnet, V., Fauteux, D., Dumont, M., and Barrere, M.: Snow physical properties may be a
 significant determinant of lemming population dynamics in the high Arctic, *Arctic Science*, 4, 813–826,
<https://doi.org/10.1139/as-2018-0008>, 2018.
- 745 Domine, F., Barrere, M., and Sarrazin, D.: Seasonal evolution of the effective thermal conductivity of the snow and the soil
 in high Arctic herb tundra at Bylot Island, Canada, *The Cryosphere*, 10, 2573–2588, [https://doi.org/10.5194/tc-10-2573-](https://doi.org/10.5194/tc-10-2573-2016)
 2016, 2016a.
- Domine, F., Barrere, M., and Morin, S.: The growth of shrubs on high Arctic tundra at Bylot Island: impact on snow
 physical properties and permafrost thermal regime, *Biogeosciences*, 13, 6471–6486, [https://doi.org/10.5194/bg-13-6471-](https://doi.org/10.5194/bg-13-6471-2016)
 750 2016, 2016b.
- Essery, R., Kontu, A., Lemmetyinen, J., Dumont, M., and Ménard, C. B.: A 7-year dataset for driving and evaluating snow
 models at an Arctic site (Sodankylä, Finland), *Geosci. Instrum. Method. Data Syst.*, 5, 219–227,
<https://doi.org/10.5194/gi-5-219-2016>, 2016.
- Gascon, G., Sharp, M., Burgess, D., Bezeau, P., Bush, A. B., Morin, S., and Lafaysse, M.: How well is firn densification
 755 represented by a physically based multilayer model? Model evaluation for Devon Ice Cap, Nunavut, Canada, *J. Glaciol.*,
 60, 694–704, <https://doi.org/10.3189/2014JoG13J209>, 2014.
- Gouttevin, I., Langer, M., Löwe, H., Boike, J., Proksch, M., and Schneebeli, M.: Observation and modelling of snow at a
 polygonal tundra permafrost site: spatial variability and thermal implications, *The Cryosphere*, 12, 3693–3717,
<https://doi.org/10.5194/tc-12-3693-2018>, 2018.
- 760 Hall, A.: The Role of Surface Albedo Feedback in Climate, *J. Climate*, 17, 1550–1568, [https://doi.org/10.1175/1520-](https://doi.org/10.1175/1520-0442(2004)017<1550:TROSAF>2.0.CO;2)
 0442(2004)017<1550:TROSAF>2.0.CO;2, 2004.
- Hersbach, H., Bell, B., Berrisford, P., Hirahara, S., Horányi, A., Muñoz-Sabater, J., Nicolas, J., Peubey, C., Radu, R.,
 Schepers, D., Simmons, A., Soci, C., Abdalla, S., Abellan, X., Balsamo, G., Bechtold, P., Biavati, G., Bidlot, J.,
 Bonavita, M., Chiara, G., Dahlgren, P., Dee, D., Diamantakis, M., Dragani, R., Flemming, J., Forbes, R., Fuentes, M.,
 765 Geer, A., Haimberger, L., Healy, S., Hogan, R. J., Hólm, E., Janisková, M., Keeley, S., Laloyaux, P., Lopez, P., Lupu,
 C., Radnoti, G., Rosnay, P., Rozum, I., Vamborg, F., Villaume, S., and Thépaut, J.-N.: The ERA5 Global Reanalysis, *Q
 J R Meteorol Soc*, <https://doi.org/10.1002/qj.3803>, 2020.
- Howat, I., Negrete, A., and Smith, B.: MEaSUREs Greenland Ice Mapping Project (GIMP) Digital Elevation Model,
 Version 1. gimpdem5_5_v01.1., NASA National Snow and Ice Data Center Distributed Active Archive Center.,
 770 <https://doi.org/10.5067/NV34YUIXLP9W>, last access: 29 July 2020, 2015.
- Howat, I. M., Negrete, A., and Smith, B. E.: The Greenland Ice Mapping Project (GIMP) land classification and surface
 elevation data sets, *The Cryosphere*, 8, 1509–1518, <https://doi.org/10.5194/tc-8-1509-2014>, 2014.



- Jacobi, H.-W., Domine, F., Simpson, W. R., Douglas, T. A., and Sturm, M.: Simulation of the specific surface area of snow using a one-dimensional physical snowpack model: implementation and evaluation for subarctic snow in Alaska, *The Cryosphere*, 4, 35–51, <https://doi.org/10.5194/tc-4-35-2010>, 2010.
- Jennings, K. S., Winchell, T. S., Livneh, B., and Molotch, N. P.: Spatial variation of the rain-snow temperature threshold across the Northern Hemisphere, *Nature communications*, 9, 1148, <https://doi.org/10.1038/s41467-018-03629-7>, 2018.
- Jordan, R. E., Andreas, E. L., and Makshtas, A. P.: Heat budget of snow-covered sea ice at North Pole 4, *J. Geophys. Res.*, 104, 7785–7806, <https://doi.org/10.1029/1999JC900011>, 1999.
- King, J., Howell, S., Brady, M., Toose, P., Derksen, C., Haas, C., and Beckers, J.: Local-scale variability of snow density on Arctic sea ice, *The Cryosphere*, 14, 4323–4339, <https://doi.org/10.5194/tc-14-4323-2020>, 2020.
- Lefebvre, F., Fettweis, X., Gallee, H., van Ypersele, J.-P., Marbaix, P., Greuell, W., and Calanca, P.: Evaluation of a high-resolution regional climate simulation over Greenland, *Clim Dyn*, 25, 99–116, <https://doi.org/10.1007/s00382-005-0005-8>, 2005.
- Libois, Q., Picard, G., France, J. L., Arnaud, L., Dumont, M., Carmagnola, C. M., and King, M. D.: Influence of grain shape on light penetration in snow, *The Cryosphere*, 7, 1803–1818, <https://doi.org/10.5194/tc-7-1803-2013>, 2013.
- Libois, Q., Picard, G., Arnaud, L., Morin, S., and Brun, E.: Modeling the impact of snow drift on the decameter-scale variability of snow properties on the Antarctic Plateau, *J. Geophys. Res. Atmos.*, 119, 11,662–11,681, <https://doi.org/10.1002/2014JD022361>, 2014.
- Liston, G. E. and Elder, K.: A Distributed Snow-Evolution Modeling System (SnowModel), *J. Hydrometeor*, 7, 1259–1276, <https://doi.org/10.1175/JHM548.1>, 2006.
- Liston, G. E. and Sturm, M.: Winter Precipitation Patterns in Arctic Alaska Determined from a Blowing-Snow Model and Snow-Depth Observations, *J. Hydrometeor*, 3, 646–659, [https://doi.org/10.1175/1525-7541\(2002\)003<0646:WPPIAA>2.0.CO;2](https://doi.org/10.1175/1525-7541(2002)003<0646:WPPIAA>2.0.CO;2), 2002.
- Liston, G. E., Perham, C. J., Shideler, R. T., and Cheuvront, A. N.: Modeling snowdrift habitat for polar bear dens, *Ecological Modelling*, 320, 114–134, <https://doi.org/10.1016/j.ecolmodel.2015.09.010>, 2016.
- Liston, G. E., Haehnel, R. B., Sturm, M., Hiemstra, C. A., Berezovskaya, S., and Tabler, R. D.: Simulating complex snow distributions in windy environments using SnowTran-3D, *J. Glaciol.*, 53, 241–256, <https://doi.org/10.3189/172756507782202865>, 2007.
- Loew, A., Bell, W., Brocca, L., Bulgin, C. E., Burdanowitz, J., Calbet, X., Donner, R. V., Ghent, D., Gruber, A., Kaminski, T., Kinzel, J., Klepp, C., Lambert, J.-C., Schaepman-Strub, G., Schröder, M., and Verhoelst, T.: Validation practices for satellite-based Earth observation data across communities, *Rev. Geophys.*, 55, 779–817, <https://doi.org/10.1002/2017RG000562>, 2017.
- Ludwig, V., Spreen, G., Haas, C., Istomina, L., Kauker, F., and Murashkin, D.: The 2018 North Greenland polynya observed by a newly introduced merged optical and passive microwave sea-ice concentration dataset, *The Cryosphere*, 13, 2051–2073, <https://doi.org/10.5194/tc-13-2051-2019>, 2019.



- Luijting, H., Vikhamar-Schuler, D., Aspelien, T., Bakketun, Å., and Homleid, M.: Forcing the SURFEX/Crocus snow model with combined hourly meteorological forecasts and gridded observations in southern Norway, *The Cryosphere*, 12, 2123–2145, <https://doi.org/10.5194/tc-12-2123-2018>, 2018.
- 810 Magnus, G.: Versuche über die Spannkkräfte des Wasserdampfs, *Annalen der Physik*, 137, 225–247, 1844.
- Maslanik, J. and Stroeve, J.: Near-Real-Time DMSP SSMIS Daily Polar Gridded Sea Ice Concentrations, Version 1. 2018-03-15., <https://doi.org/10.5067/U8C09DWVX9LM>, <https://nsidc.org/data/NSIDC-0081/versions/1>, last access: 24 February 2021.
- Meister, R.: Density of New Snow and its Dependence on Air Temperature and Wind. Correction of Precipitation
 815 Measurements, *Zürcher Geographische Schriften*, 1985.
- Minola, L., Zhang, F., Azorin-Molina, C., Pirooz, A. A. S., Flay, R. G. J., Hersbach, H., and Chen, D.: Near-surface mean and gust wind speeds in ERA5 across Sweden: towards an improved gust parametrization, *Clim Dyn*, 55, 887–907, <https://doi.org/10.1007/s00382-020-05302-6>, 2020.
- Moore, G. W. K., Schweiger, A., Zhang, J., and Steele, M.: What Caused the Remarkable February 2018 North Greenland
 820 Polynya?, *Geophysical Research Letters*, 45, 13,342–13,350, <https://doi.org/10.1029/2018GL080902>, 2018.
- Pedersen, S. H., Tamstorf, M. P., Abermann, J., Westergaard-Nielsen, A., Lund, M., Skov, K., Sigsgaard, C., Mylius, M. R., Hansen, B. U., and Liston, G. E.: Spatiotemporal characteristics of seasonal snow cover in Northeast Greenland from in situ observations, *Arctic, Antarctic, and Alpine Research*, 48, 653–671, <https://doi.org/10.1657/AAAR0016-028>, 2016.
- Proksch, M., Löwe, H., and Schneebeli, M.: Density, specific surface area, and correlation length of snow measured by high-
 825 resolution penetrometry, *J. Geophys. Res. Earth Surf.*, 120, 346–362, <https://doi.org/10.1002/2014JF003266>, 2015.
- Rasch, M., Frandsen, E. R., Skov, H., and Hansen, J. L.: Site Manual. Villum Research Station. Station Nord. Greenland, https://villumresearchstation.dk/fileadmin/villumresearchstation/Generelle/SITE_MANUAL.pdf, last access: 28 May 2020, 2016.
- Sauter, T. and Obleitner, F.: Assessing the uncertainty of glacier mass-balance simulations in the European Arctic based on
 830 variance decomposition, *Geoscientific Model Development*, 8, 3911–3928, <https://doi.org/10.5194/gmd-8-3911-2015>, 2015.
- Schmidt, N. M., Ims, R. A., Høye, T. T., Gilg, O., Hansen, L. H., Hansen, J., Lund, M., Fuglei, E., Forchhammer, M. C., and Sittler, B.: Response of an arctic predator guild to collapsing lemming cycles, *Proceedings. Biological sciences*, 279, 4417–4422, <https://doi.org/10.1098/rspb.2012.1490>, 2012.
- 835 Schneebeli, M., Pielmeier, C., and Johnson, J. B.: Measuring snow microstructure and hardness using a high resolution penetrometer, *Cold Regions Science and Technology*, 30, 101–114, [https://doi.org/10.1016/S0165-232X\(99\)00030-0](https://doi.org/10.1016/S0165-232X(99)00030-0), 1999.
- Stiegler, C., Lund, M., Christensen, T. R., Mastepanov, M., and Lindroth, A.: Two years with extreme and little snowfall: effects on energy partitioning and surface energy exchange in a high-Arctic tundra ecosystem, *The Cryosphere*, 10, 840 1395–1413, <https://doi.org/10.5194/tc-10-1395-2016>, 2016.



- Sturm, M., Holmgren, J., König, M., and Morris, K.: The thermal conductivity of seasonal snow, *J. Glaciol.*, 43, 26–41, <https://doi.org/10.3189/S0022143000002781>, 1997.
- Tuzet, F., Dumont, M., Lafaysse, M., Picard, G., Arnaud, L., Voisin, D., Lejeune, Y., Charrois, L., Nabat, P., and Morin, S.: A multilayer physically based snowpack model simulating direct and indirect radiative impacts of light-absorbing impurities in snow, *The Cryosphere*, 11, 2633–2653, <https://doi.org/10.5194/tc-11-2633-2017>, 2017.
- Tuzet, F., Dumont, M., Picard, G., Lamare, M., Voisin, D., Nabat, P., Lafaysse, M., Larue, F., Revuelto, J., and Arnaud, L.: Quantification of the radiative impact of light-absorbing particles during two contrasted snow seasons at Col du Lautaret (2058 m a.s.l., French Alps), *The Cryosphere*, 14, 4553–4579, <https://doi.org/10.5194/tc-14-4553-2020>, 2020.
- Uotila, P., Goosse, H., Haines, K., Chevallier, M., Barthélemy, A., Bricaud, C., Carton, J., Fučkar, N., Garric, G., Iovino, D., Kauker, F., Korhonen, M., Lien, V. S., Marnela, M., Massonnet, F., Mignac, D., Peterson, K. A., Sadikni, R., Shi, L., Tietsche, S., Toyoda, T., Xie, J., and Zhang, Z.: An assessment of ten ocean reanalyses in the polar regions, *Clim Dyn.*, 52, 1613–1650, <https://doi.org/10.1007/s00382-018-4242-z>, 2019.
- Urraca, R., Huld, T., Gracia-Amillo, A., Martinez-de-Pison, F. J., Kaspar, F., and Sanz-Garcia, A.: Evaluation of global horizontal irradiance estimates from ERA5 and COSMO-REA6 reanalyses using ground and satellite-based data, *Solar Energy*, 164, 339–354, <https://doi.org/10.1016/J.SOLENER.2018.02.059>, 2018.
- Van Kampenhout, L., Lenaerts, J. T. M., Lipscomb, W. H., Sacks, W. J., Lawrence, D. M., Slater, A. G., and van den Broeke, M. R.: Improving the Representation of Polar Snow and Firn in the Community Earth System Model, *J. Adv. Model. Earth Syst.*, 9, 2583–2600, <https://doi.org/10.1002/2017MS000988>, 2017.
- Villum Reserach Station: Meteorological Data, Asiaqmet, <https://www2.dmu.dk/asiaqmet/Default.aspx>, last access: 5 February 2021, 2021.
- Vionnet, V., Guyomarc’h, G., Naaïm Bouvet, F., Martin, E., Durand, Y., Bellot, H., Bel, C., and Pugliese, P.: Occurrence of blowing snow events at an alpine site over a 10-year period: Observations and modelling, *Advances in Water Resources*, 55, 53–63, <https://doi.org/10.1016/j.advwatres.2012.05.004>, 2013.
- Vionnet, V., Brun, E., Morin, S., Boone, A., Faroux, S., Le Moigne, P., Martin, E., and Willemet, J.-M.: The detailed snowpack scheme Crocus and its implementation in SURFEX v7.2, *Geosci. Model Dev.*, 5, 773–791, <https://doi.org/10.5194/gmd-5-773-2012>, 2012.
- Wang, C., Graham, R. M., Wang, K., Gerland, S., and Granskog, M. A.: Comparison of ERA5 and ERA-Interim near-surface air temperature, snowfall and precipitation over Arctic sea ice: effects on sea ice thermodynamics and evolution, *The Cryosphere*, 13, 1661–1679, <https://doi.org/10.5194/TC-13-1661-2019>, 2019.
- Wang, Z.: The Solar Resource and Meteorological Parameters, in: *Design of solar thermal power plants*, edited by: Wang, Z., Elsevier, 47–115, <https://doi.org/10.1016/B978-0-12-815613-1.00002-X>, 2019.
- Willett, K. M., Jones, P. D., Gillett, N. P., and Thorne, P. W.: Recent Changes in Surface Humidity: Development of the HadCRUH Dataset, *J. Climate*, 21, 5364–5383, <https://doi.org/10.1175/2008JCLI2274.1>, 2008.
- Yankee Environmental Systems: TPS_3100 Total Precipitation Sensor. Installation & User Guide Version 2.01, 2012.



- 875 Zuanon, N. (Ed.): IceCube, a portable and reliable instrument for snow specific surface area measurement in the field, 1020-1023, 2013.